

Manuscript Number: CEJ-D-18-06459R1

Title: Tailoring the structure of Co-Mo/mesoporous  $\gamma$ -Al<sub>2</sub>O<sub>3</sub> catalysts by adding multi-hydroxyl compound: A 3000 kt/a industrial-scale diesel ultra-deep hydrodesulfurization study

Article Type: SI:ISCRE 25

Keywords: hydrodesulfurization; diesel; structure manipulation; Co-Mo/mesoporous Al<sub>2</sub>O<sub>3</sub>; industrial-scale

Corresponding Author: Professor xiangchen fang, Prof. Dr.

Corresponding Author's Institution: East China University of Science and Technology

First Author: Chong Peng

Order of Authors: Chong Peng; Rong Guo; Xiang Feng; xiangchen fang, Prof. Dr.

Abstract: Ever-increasing concern on environmental impacts (e.g., sulfur pollution) by fossil fuels has triggered the research on hydrodesulfurization (HDS). In this work, Co-Mo nanoparticles were deposited on the mesoporous  $\gamma$ -Al<sub>2</sub>O<sub>3</sub> support with the addition of organic compound, and the physico-chemical properties of the catalysts (Co-Mo-C/mesoporous  $\gamma$ -Al<sub>2</sub>O<sub>3</sub>) were then characterized by multi-techniques such as H<sub>2</sub>-TPR, HRTEM, XPS, N<sub>2</sub> physisorption. It is found that the Co-Mo-C/mesoporous  $\gamma$ -Al<sub>2</sub>O<sub>3</sub> catalyst is easier to be reduced when organic compound is added, enhancing the sulfuration. This results in better dispersion of Co-Mo-S species and more Co-Mo-S II active sites, which significantly enhance diesel ultra-deep hydrodesulfurization activity. Furthermore, this novel catalyst was also tested for HDS reaction in a 3000 kt/a industrial-scale plant. Gratifyingly, this catalyst showed effective reduction of sulfur content from 9000 to less than 10  $\mu$ g/g and also high stability over 5000 h. The results are of great significance to the design and development of industrial HDS catalysts.

Response to Reviewers: Thank you very much for your valuable comments and suggestions. We tried our best to improve the manuscript and made the changes in the revised version. We hope that the corrections will meet with approval.

Reviewer #1:

Controlling and decreasing the environmental impacts of fossil fuels on the environment and human shows great scientific and industrial importance. This paper deals with the quite essential topic of eliminating sulfur heteroatom in fossil fuels processing. The authors developed the multi-hydroxyl compound promoted Co-Mo/Al<sub>2</sub>O<sub>3</sub> catalyst, and elucidated the effect of multi-hydroxyl compound on catalyst structure and performance for diesel ultra-deep hydrodesulfurization. The characterizations and discussions convincingly demonstrate the structure-performance relationship. Moreover, the

promoted catalyst can be even used in 3000kt/a industrial process, which is of great referential significance to the design of other HDS catalysts. Therefore, this paper is written in good English and can be accepted for publication after the following revision.

Response:

Thanks for the good comments on the quality of our manuscript.

1) For diesel HDS catalyst, the pore structure of support should also be essential to the catalytic performance. Please add discussion on the role of support in HDS reactions to better improve this paper.

Response:

It is true as the reviewer mentioned that pore structure of support is essential.

In order to better improve this paper, we added the following discussion in the revised manuscript: "Al<sub>2</sub>O<sub>3</sub> in  $\alpha$  and  $\gamma$  forms is the most common support for HDS catalysts because of its outstanding textural and mechanical properties. Normally, these properties can be easily tuned based on the detailed reaction requirements, feedstock compositions and product's targeted specifications." and "Among the structural and textural properties, pore size is extremely essential because the diffusion of different species inside pores of Al<sub>2</sub>O<sub>3</sub> could affect and limit the HDS overall reaction rate".

2) In experimental section, the TPD and Py-IR conditions should be added.

Response:

Thanks for the kind suggestion.

In the revised manuscript, we have added the details of TPD and Py-IR as follows: "NH<sub>3</sub>-TPD was conducted as follows: the catalysts after calcination were saturated with NH<sub>3</sub> for 30 min at 100°C. Afterwards, He was flushed to remove the physically adsorbed molecules. The TPD results were collected in He from 323 to 873 K with a heating rate of 10 K/min. Py-adsorbed IR spectra were recorded on a PE FTIR Frontier instrument. The system was degassed at 500 °C for 5 h under vacuum and flushed by pure pyridine at room temperature for 20 min. The infrared (IR) spectra were then recorded."

Again, thanks for the careful review by the reviewer.

3) More details of catalytic evaluation process in industrial scale should be given to better guide the readers.

Response:

To help readers better understand our results, we have added the following details in the revised manuscript as follows: "The feedstock was pumped into the furnace, and was heated first through heat exchanger. The heated feedstock was then introduced into the reactor. After reaction, the final products were separated by high-pressure and low-pressure separators".

4) The resolution of Figure 1 is not high enough, which should be improved.

Response:

Thanks for the careful review by the reviewer. The new figure 1 with high resolution has been added in the revised manuscript.

Reviewer #2:

This article described a novel method to tailor the micro-structure and catalytic performance of diesel HDS catalysts via the addition of glycerol into the impregnation solution. Interestingly, the authors found that this simple method could lead to the fine tuning of the

resulting Co-Mo-S active phase in terms of slab size and dispersion, and accordingly the catalyst prepared with the addition of glycerol exhibited much better catalytic performance in diesel HDS. More importantly, the authors demonstrated that the resulting catalyst has been commercially used for 3 years in a 3000 kt/a industrial unit. I recommend this article for publication in CEJ after the following revisions in addition to those I have marked in the pdf document:

Response:

Thanks for the good comments on the quality of our manuscript.

1) The authors systematically characterized the physicochemical properties of the two catalysts prepared with and without the addition of glycerol, but they did not give any interpretation in the changes of the active phase structures such as increased stacking and dispersion and decreased size.

Response:

Thanks for the suggestion by the reviewer. In order to make our results better understood by the readers, we have modified the corresponding discussion in the revised manuscript: "The results show that the addition of compound decrease the interaction between metal and support.

Therefore, the average length reduces and the dispersion increases." and "The addition of organic compound leads to increased acidity and weaker metal-support interaction. This enhances the sulfuration and generates more type II Co-Mo-S active phase".

2) In the bottom of Page 9, the authors stated that "It can be seen from Table 1 that total acid sites together with B/L ratio are all larger on Co-Mo-C/mesoporous  $\gamma$ -Al<sub>2</sub>O<sub>3</sub> than those on Co-Mo/mesoporous  $\gamma$ -Al<sub>2</sub>O<sub>3</sub> catalyst, which could greatly affect the HDS reaction." What is the reason for the different acidity of the two catalysts? What is the role glycerol played in changing the acidity?

Response:

Thanks for the careful review. Normally, the multi-hydroxyl compound could interact with the metal to form a complex, which increases the Brønsted acid sites of the catalyst. This is also in accordance with previous results (Journal of Catalysis 330 (2015) 374-386).

In order the better improve this manuscript, we also added the following discussion in the revised version: "It can be seen from Table 1 that total acid sites together with B/L ratio are all larger on Co-Mo-C/mesoporous  $\gamma$ -Al<sub>2</sub>O<sub>3</sub> than those on Co-Mo/mesoporous  $\gamma$ -Al<sub>2</sub>O<sub>3</sub> catalyst, possibly due to the formation of complex between metal and multi-hydroxyl compound".

3) A relevant question to Question 2 is that increased acidity usually give rise to serious carbon deposition, how do they two catalysts differ in carbon deposition?

Response:

Thanks for the comments by the reviewer. It is reported that Lewis acid sites normally involve in the coke deposition (J. Catal. 299 (2013) 321-335; Fuel Process. Tech. 9 (1984) 103-108). The Lewis of Co-Mo-C/mesoporous  $\gamma$ -Al<sub>2</sub>O<sub>3</sub> catalyst with multi-hydroxyl compound addition is smaller. Therefore, the coke formation of Co-Mo-C/mesoporous  $\gamma$ -Al<sub>2</sub>O<sub>3</sub> catalyst is alleviated to less than commercial Co-Mo/mesoporous  $\gamma$ -Al<sub>2</sub>O<sub>3</sub> catalyst. This is also confirmed by the high HDS stability (Figure 5).

4) The English of this article should be further polished.

Response:

Thanks for the kind suggestion. We have carefully polished the English of this manuscript. We think it is now suitable for publication.

We have tried our best to improve the manuscript. Thanks to the constructive comments and suggestions from the two reviewers, we have made corresponding changes in the revised version. These changes will not influence the framework of the paper. Once again, we appreciate your valuable comments and suggestions very much and hope that the correction will meet with approval.

SINOPEC Dalian Institute of Petroleum and Petrochemicals

East China University of Science and Technology

E-mail: fxc@ecust.edu.cn

Tel.: +86-0411-39699409 Fax. : +86-24-56429551



Dear Prof. Enrico Tronconi,

On behalf of my co-authors, we thank you very much for your efforts in our manuscript and the minor revision decision. We also appreciate the reviewers very much for their constructive comments and valuable suggestions on our manuscript entitled “*Tailoring the structure of Co-Mo/mesoporous  $\gamma$ -Al<sub>2</sub>O<sub>3</sub> catalysts by adding multi-hydroxyl compound: A 3000 kt/a industrial-scale diesel ultra-deep hydrodesulfurization study*”. (ID: CEJ-D-18-06459).

We have studied reviewers’ comments carefully and have made all revisions required by reviewers. Attached please find the revised version, which we would like to submit for your kind consideration. Looking forward to hearing from you.

Thank you and best regards.

Sincerely yours

Xiangchen Fang

List of potential reviewers:

1) **Prof. Xiaojun Bao**

Fuzhou University, Fujian, China

E-mail: baoxj@fzu.edu.cn

Prof. Bao is an expert in hydrodesulphurization catalysis. His review will be helpful to improve the quality of the paper.

2) **Prof. Jinsen Gao**

State Key Laboratory of Heavy Oil Processing, Beijing, China

E-mail: jsgao@cup.edu.cn

Prof. Gao is an expert in hydrotreating of fuel and has published many papers in related research field.

3) **Prof. Zhigang Lei**

State Key Laboratory of Chemical Resource Engineering, Beijing University of Chemical Technology, Beijing, China

E-mail: leizhg@mail.buct.edu.cn

Prof. Lei is an expert in sulfur removal and published many papers in this research field.

Thank you very much for your valuable comments and suggestions. We tried our best to improve the manuscript and made the changes in the revised version. We hope that the corrections will meet with approval.

**Reviewer #1:**

Controlling and decreasing the environmental impacts of fossil fuels on the environment and human shows great scientific and industrial importance. This paper deals with the quite essential topic of eliminating sulfur heteroatom in fossil fuels processing.

The authors developed the multi-hydroxyl compound promoted Co-Mo/Al<sub>2</sub>O<sub>3</sub> catalyst, and elucidated the effect of multi-hydroxyl compound on catalyst structure and performance for diesel ultra-deep hydrodesulfurization. The characterizations and discussions convincingly demonstrate the structure-performance relationship. Moreover, the promoted catalyst can be even used in 3000kt/a industrial process, which is of great referential significance to the design of other HDS catalysts. Therefore, this paper is written in good English and can be accepted for publication after the following revision.

**Response:**

Thanks for the good comments on the quality of our manuscript.

1) For diesel HDS catalyst, the pore structure of support should also be essential to the catalytic performance. Please add discussion on the role of support in HDS reactions to better improve this paper.

**Response:**

It is true as the reviewer mentioned that pore structure of support is essential.

In order to better improve this paper, we added the following discussion in the revised manuscript: “Al<sub>2</sub>O<sub>3</sub> in  $\alpha$  and  $\gamma$  forms is the most common support for HDS catalysts because of its outstanding textural and mechanical properties. Normally, these properties can be easily tuned based on the detailed reaction requirements, feedstock compositions and product’s targeted

specifications.” and “Among the structural and textural properties, pore size is extremely essential because the diffusion of different species inside pores of Al<sub>2</sub>O<sub>3</sub> could affect and limit the HDS overall reaction rate”.

2) In experimental section, the TPD and Py-IR conditions should be added.

Response:

Thanks for the kind suggestion.

In the revised manuscript, we have added the details of TPD and Py-IR as follows:

“NH<sub>3</sub>-TPD was conducted as follows: the catalysts after calcination were saturated with NH<sub>3</sub> for 30 min at 100°C. Afterwards, He was flushed to remove the physically adsorbed molecules. The TPD results were collected in He from 323 to 873 K with a heating rate of 10 K/min. Py-adsorbed IR spectra were recorded on a PE FTIR Frontier instrument. The system was degassed at 500 °C for 5 h under vacuum and flushed by pure pyridine at room temperature for 20 min. The infrared (IR) spectra were then recorded.”

Again, thanks for the careful review by the reviewer.

3) More details of catalytic evaluation process in industrial scale should be given to better guide the readers.

Response:

To help readers better understand our results, we have added the following details in the revised manuscript as follows: “The feedstock was pumped into the furnace, and was heated first through heat exchanger. The heated feedstock was then introduced into the reactor. After reaction, the final products were separated by high-pressure and low-pressure separators”.

4) The resolution of Figure 1 is not high enough, which should be improved.

Response:

Thanks for the careful review by the reviewer. The new figure 1 with high resolution has been added in the revised manuscript.



## Reviewer #2:

This article described a novel method to tailor the micro-structure and catalytic performance of diesel HDS catalysts via the addition of glycerol into the impregnation solution. Interestingly, the authors found that this simple method could lead to the fine tuning of the resulting Co-Mo-S active phase in terms of slab size and dispersion, and accordingly the catalyst prepared with the addition of glycerol exhibited much better catalytic performance in diesel HDS. More importantly, the authors demonstrated that the resulting catalyst has been commercially used for 3 years in a 3000 kt/a industrial unit. I recommend this article for publication in CEJ after the following revisions in addition to those I have marked in the pdf document:

### Response:

Thanks for the good comments on the quality of our manuscript.

1) The authors systematically characterized the physicochemical properties of the two catalysts prepared with and without the addition of glycerol, but they did not give any interpretation in the changes of the active phase structures such as increased stacking and dispersion and decreased size.

### Response:

Thanks for the suggestion by the reviewer. In order to make our results better understood by the readers, we have modified the corresponding discussion in the revised manuscript: “The results show that the addition of compound decrease the interaction between metal and support. Therefore, the average length reduces and the dispersion increases.” and “The addition of organic compound leads to increased acidity and weaker metal-support interaction. This enhances the sulfuration and generates more type II Co-Mo-S active phase”.

2) In the bottom of Page 9, the authors stated that "It can be seen from Table 1 that total acid sites together with B/L ratio are all larger on Co-Mo-C/mesoporous  $\gamma$ -Al<sub>2</sub>O<sub>3</sub> than those on Co-Mo/mesoporous  $\gamma$ -Al<sub>2</sub>O<sub>3</sub> catalyst, which could greatly affect the HDS reaction." What is the reason for the different acidity of the two catalysts? What is the role glycerol played in changing the acidity?

Response:

Thanks for the careful review. Normally, the multi-hydroxyl compound could interact with the metal to form a complex, which increases the Brønsted acid sites of the catalyst. This is also in accordance with previous results (*Journal of Catalysis* 330 (2015) 374–386).

In order to better improve this manuscript, we also added the following discussion in the revised version: “It can be seen from Table 1 that total acid sites together with B/L ratio are all larger on Co-Mo-C/mesoporous  $\gamma$ -Al<sub>2</sub>O<sub>3</sub> than those on Co-Mo/mesoporous  $\gamma$ -Al<sub>2</sub>O<sub>3</sub> catalyst, possibly due to the formation of complex between metal and multi-hydroxyl compound”.

3) A relevant question to Question 2 is that increased acidity usually give rise to serious carbon deposition, how do they two catalysts differ in carbon deposition?

Response:

Thanks for the comments by the reviewer. It is reported that Lewis acid sites normally involve in the coke deposition (*J. Catal.* 299 (2013) 321–335; *Fuel Process. Tech.* 9 (1984) 103-108). The Lewis of Co-Mo-C/mesoporous  $\gamma$ -Al<sub>2</sub>O<sub>3</sub> catalyst with multi-hydroxyl compound addition is smaller. Therefore, the coke formation of Co-Mo-C/mesoporous  $\gamma$ -Al<sub>2</sub>O<sub>3</sub> catalyst is alleviated, as shown in the following figure 1. This is also confirmed by the high HDS stability (Figure 5).

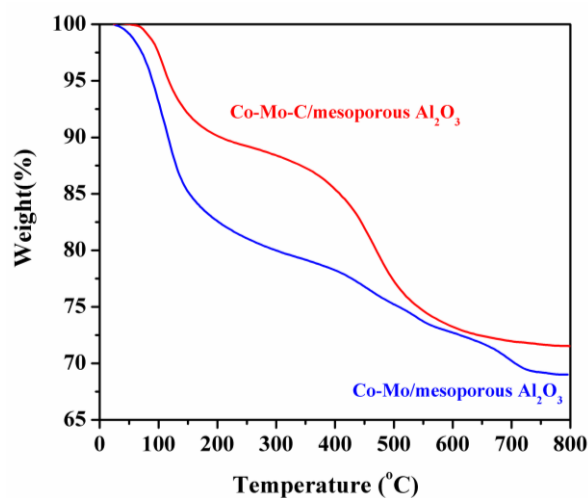


Figure 1. TGA results of Co-Mo/Mesoporous Al<sub>2</sub>O<sub>3</sub> and Co-Mo-C/Mesoporous Al<sub>2</sub>O<sub>3</sub> catalysts.

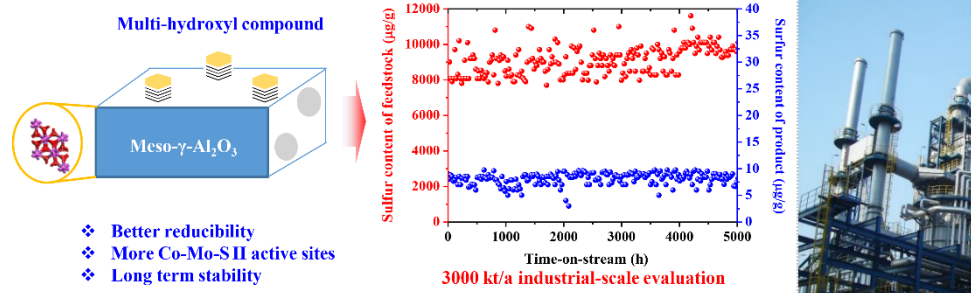
4) The English of this article should be further polished.

Response:

Thanks for the kind suggestion. We have carefully polished the English of this manuscript. We think it is now suitable for publication.

We have tried our best to improve the manuscript. Thanks to the constructive comments and suggestions from the two reviewers, we have made corresponding changes in the revised version. These changes will not influence the framework of the paper. Once again, we appreciate your valuable comments and suggestions very much and hope that the correction will meet with approval.

Graphical abstract:



**Highlights:**

- ❖ Co-Mo nanoparticles are impregnated with the addition of multi-hydroxyl compound.
- ❖ Co-Mo-C/mesoporous  $\gamma$ -Al<sub>2</sub>O<sub>3</sub> catalyst is easier to be reduced.
- ❖ More Co-Mo-S type II sites exist due to weak metal-support interaction.
- ❖ 99.9% sulfur removal activity is achieved over 5000 h in a 3000kt/a industrial plant.

**Supplementary Material**

[Click here to download Supplementary Material: Supporting information.docx](#)

1  
2  
3  
4  
5  
6  
7  
8  
9  
10  
11  
12  
13  
14  
15  
16  
17  
18  
19  
20  
21  
22  
23  
24  
25  
26  
27  
28  
29  
30  
31  
32  
33  
34  
35  
36  
37  
38  
39  
40  
41  
42  
43  
44  
45  
46  
47  
48  
49  
50  
51  
52  
53  
54  
55  
56  
57  
58  
59  
60  
61  
62  
63  
64  
65

# Tailoring the structure of Co-Mo/mesoporous $\gamma$ -Al<sub>2</sub>O<sub>3</sub> catalysts by adding multi-hydroxyl compound: A 3000 kt/a industrial-scale diesel ultra-deep hydrodesulfurization study

Chong Peng<sup>†</sup>, Rong Guo<sup>†</sup>, Xiang Feng<sup>\*\*</sup> and Xiangchen Fang<sup>\*\*</sup>

<sup>†</sup> Dalian Research Institute of Petroleum and Petrochemicals, SINOPEC, Dalian 116045, China

<sup>\*\*</sup> State Key Laboratory of Heavy Oil Processing, China University of Petroleum, Qingdao 266580, China

**Abstract:** Ever-increasing concern on environmental impacts (e.g., sulfur pollution) by fossil fuels has triggered the research on hydrodesulfurization (HDS). In this work, Co-Mo nanoparticles were deposited on the mesoporous  $\gamma$ -Al<sub>2</sub>O<sub>3</sub> support with the addition of organic compound, and the physico-chemical properties of the catalysts (Co-Mo-C/mesoporous  $\gamma$ -Al<sub>2</sub>O<sub>3</sub>) were then characterized by multi-techniques such as H<sub>2</sub>-TPR, HRTEM, XPS, N<sub>2</sub> physisorption. It is found that the Co-Mo-C/mesoporous  $\gamma$ -Al<sub>2</sub>O<sub>3</sub> catalyst is easier to be reduced when organic compound is added, enhancing the sulfuration. This results in better dispersion of Co-Mo-S species and more Co-Mo-S II active sites, which significantly enhance diesel ultra-deep hydrodesulfurization activity. Furthermore, this novel catalyst was also tested for HDS reaction in a 3000 kt/a industrial-scale plant. Gratifyingly, this catalyst showed effective reduction of sulfur content from 9000 to less than 10  $\mu$ g/g and also high stability over 5000 h. The results are of great significance to the design and development of industrial HDS catalysts.

**Keywords:** hydrodesulfurization; diesel; structure manipulation; Co-Mo/mesoporous Al<sub>2</sub>O<sub>3</sub>; industrial-scale

# 1. Introduction

Growing concern on environment necessitates the elimination of heteroatoms such as sulfur and nitrogen from fossil fuels. This worldwide demand for clean fuels leads to strict legislation to control and decrease the environmental impacts of fossil fuels on the environment and human beings. For example, Euro V standard of diesel fuel strictly requires that the diesel sulfur content is less than 10 ppm[1]. However, the removal of refractive sulfur-containing alkyl derivatives of dibenzothiophene (DBTs)[2], such as 4-dimethyldibenzothiophene (4-MDBT) and 4,6-dimethyldibenzothiophene (4,6-DMDBT), is quite challenging. Ultra-deep hydrodesulfurization (HDS) to produce ultra-low-sulfur[3] diesel fuels with sulfur content of less than 10 ppm is one of the most essential industrial processes to resolve the above problem[4-6]. This has triggered the great attention of researchers on developing highly efficient catalysts for HDS [7-11].

The most important HDS catalyst used in oil refineries is usually the Co(Ni)Mo/Al<sub>2</sub>O<sub>3</sub> catalysts [12-14]. The structure of the typical Co(Ni)-Mo catalyst can be briefly described by the Co(Ni)-Mo-S model, which was first reported by Topsøe[15]. The structure of catalytically active Co(Ni)-Mo-S sites is formed by the decoration of Co(Ni) atoms on the well-dispersed MoS<sub>2</sub> nanocrystals[16]. These active sites can be obtained by the sulfidation process[3]. It is widely accepted that the HDS activity and stability of the catalysts are greatly affected by the physico-chemical properties of the support and metals [1, 2]. Al<sub>2</sub>O<sub>3</sub> in  $\alpha$  and  $\gamma$  forms is the most common support for HDS catalysts because of its outstanding textural and mechanical properties. Normally, these properties can be easily tuned based on the detailed reaction requirements, feedstock compositions and product's targeted specifications[17].



1  
2  
3  
4  
5  
6  
7  
8  
9  
10  
11  
12  
13  
14  
15  
16  
17  
18  
19  
20  
21  
22  
23  
24  
25  
26  
27  
28  
29  
30  
31  
32  
33  
34  
35  
36  
37  
38  
39  
40  
41  
42  
43  
44  
45  
46  
47  
48  
49  
50  
51  
52  
53  
54  
55  
56  
57  
58  
59  
60  
61  
62  
63  
64  
65

Besides the properties of support, the interaction between the support and Co-Mo metals are usually quite essential to the design of effective HDS catalyst. It was reported that using chelating agents or additives such as P and B can reduce the interaction between active metals and aluminum supports, producing more active HDS sites [18-20]. Although much attention has been devoted to understanding the effect of support properties on HDS performance, few reports were focused on enhancing catalytic performance by manipulating the metal-support interaction aiming at industrial application. There is urgent need to design suitable catalyst for industrial HDS reaction, which is of prime scientific and industrial importance.

In this work, the effects of organic compound on catalyst structure and HDS performance are investigated, aiming at the industrial-scale HDS process development. Mesoporous  $\gamma$ -Al<sub>2</sub>O<sub>3</sub> is first employed as support, and then load Co-Mo nanoparticles with the addition of organic compound. The physico-chemical properties of the catalysts are studied by multi-techniques such as XRD, XPS, TPR, HRTEM, NH<sub>3</sub>-TPD and Py-IR. It is found that the introduction of organic compound makes the catalyst easily reduced, generating more type II Co-Mo-S active sites and enhancing the HDS activity and stability. Moreover, this catalyst is also tested in an 3000 kt/a industrial-scale HDS unit, and shows fantastic 99.9% sulfur reduction from 9000 to less than 10  $\mu$ g/g over 5000 h. The properties of the used catalyst after long-term evaluation and regeneration are further discussed. The results reported herein are of great referential importance to the design of industrial catalysts, and is expected to be extended to other HDS catalysts.

## 2. Experimental

### 2.1 Synthesis of Co-Mo/mesoporous $\gamma$ -Al<sub>2</sub>O<sub>3</sub> catalyst

The mesoporous  $\gamma$ -Al<sub>2</sub>O<sub>3</sub> support was provided by Fushun Catalysts Factory of

1 SINOPEC. Two Co-Mo catalysts were prepared by impregnation with an aqueous  
2 solution of cobalt nitrate  $[\text{Co}(\text{NO}_3)_2 \cdot 6\text{H}_2\text{O}]$  and ammonium heptamolybdate  
3  $[(\text{NH}_4)_6\text{Mo}_7\text{O}_{24} \cdot 4\text{H}_2\text{O}]$  with and without the addition of multi-hydroxyl compound. The  
4 loadings of Mo and Co oxides are 18 and 3wt%, respectively. The resultant catalysts  
5 were then dried at 110 °C and calcined at 500 °C for 3 h. The catalysts were then  
6 subjected to sulfidation. Typically, the catalyst was placed in a reactor at 4 MPa of  $\text{H}_2$   
7 and heated to 110 °C. Sulfidizing oil (96% kerosene and 4%  $\text{CS}_2$ ) was then added into  
8 the reactor and maintained for 3 h. Afterwards, the reactor was heated to 360 °C for 8 h.  
9 The resultant catalyst prepared with the addition of multi-hydroxyl compound is named  
10 as Co-Mo-C/mesoporous  $\gamma\text{-Al}_2\text{O}_3$ . For comparison, the catalyst without multi-hydroxyl  
11 compound addition is denoted as Co-Mo/mesoporous  $\gamma\text{-Al}_2\text{O}_3$ .

## 2.2 Characterizations

12  $\text{N}_2$  physisorption was performed on a Micromeritics ASAP 2020 instrument at -196  
13 °C. Each sample was heated to 300 °C under vacuum for 3 h prior to testing. The XRD  
14 patterns of the catalysts were determined on a Rigaku Miniflex powder diffractometer  
15 with  $\text{CuK}_\alpha$  radiation ( $\lambda=0.154$  nm). TPR curves were obtained on a Micromeritics  
16 AutoChem 2920 instrument to analyze the reducibility of the catalysts. All samples  
17 were calcined at 450 °C for 1 h and then heated from room temperature to 1000°C in a  
18 10%  $\text{H}_2/\text{Ar}$  mixture. XPS were performed on a Multilab2000X instrument  
19 (ThermoFisher) using  $\text{Mg-K}_\alpha$  radiation. All spectra were corrected using 284.6 eV as the  
20 reference for C1s binding energy. HRTEM measurements were conducted on a JEM-  
21 2100 instrument operating at 200 kV. The sulfur content was obtained by sulfur content  
22 analysis (ANTEK-9000) using Ar and  $\text{O}_2$  as carrier and burning gas, respectively. The  
23 analysis standard was SH/T0689-2000.  $\text{NH}_3\text{-TPD}$  was conducted as follows: the  
24 catalysts after calcination were saturated with  $\text{NH}_3$  for 30 min at 100°C. Afterwards, He

1 was flushed to remove the physically adsorbed molecules. The TPD results were  
2 collected in He from 323 to 873 K with a heating rate of 10 K/min. Py-adsorbed IR  
3 spectra were recorded on a PE FTIR Frontier instrument. The system was degassed at  
4 500 °C for 5 h under vacuum and flushed by pure pyridine at room temperature for 20  
5 min. The infrared (IR) spectra were then recorded.  
6  
7  
8  
9  
10

### 11 2.3 Catalytic testing in a 3000 kt/a industrial unit 12 13 14 15

16 The industrial-scale HDS reaction was carried out in a fixed bed reactor, and the  
17 corresponding schematic diagram is illustrated in Fig. 1. Typically, Co-Mo-  
18 C/mesoporous  $\gamma$ -Al<sub>2</sub>O<sub>3</sub> catalyst was shaped into particle with size of 1-3 mm. Both the  
19 top and bottom of the fixed bed reactor were filled with inert particles. The catalysts  
20 were loaded into reactor of  $D/d_p > 18$ ,  $L/d_p > 350$ , where D, L and  $d_p$  are the inner  
21 diameter, height of bed and catalysis particle size, respectively. The feedstock was  
22 pumped into the furnace, and was heated first through heat exchanger. The heated  
23 feedstock was then introduced into the reactor. After reaction, the final products were  
24 separated by high-pressure and low-pressure separators.  
25  
26  
27  
28  
29  
30  
31  
32  
33  
34  
35  
36  
37  
38

39 (Figure 1 should be inserted herein)  
40  
41  
42

## 43 3. Results and discussions 44 45

### 46 3.1 Effect of organic compound on catalyst structure 47 48

49 The mesoporous  $\gamma$ -Al<sub>2</sub>O<sub>3</sub> support in this work was first characterized by N<sub>2</sub>  
50 physisorption, as shown in Fig. 2a. According to the IUPAC classification, it can be  
51 seen that this support has Type IV adsorption-desorption isotherms[1, 21], revealing the  
52 mesoporous characteristic. The hysteresis loop of the isotherm starts at ~0.4, indicating  
53 that the mesopores are intracrystalline rather than intercrystalline. From the inset of Fig.  
54  
55  
56  
57  
58  
59  
60  
61  
62  
63  
64  
65

1  
2  
3  
4  
5  
6  
7  
8  
9  
10  
11  
12  
13  
14  
15  
16  
17  
18  
19  
20  
21  
22  
23  
24  
25  
26  
27  
28  
29  
30  
31  
32  
33  
34  
35  
36  
37  
38  
39  
40  
41  
42  
43  
44  
45  
46  
47  
48  
49  
50  
51  
52  
53  
54  
55  
56  
57  
58  
59  
60  
61  
62  
63  
64  
65

2a, it is observed that the mesoporous  $\gamma$ -Al<sub>2</sub>O<sub>3</sub> support has average pore size (ca. 7.8 nm). The detailed information of pore structure is summarized in Table S1. The pore volume and surface area of mesoporous  $\gamma$ -Al<sub>2</sub>O<sub>3</sub> support are normally larger than those of a typical commercial Al<sub>2</sub>O<sub>3</sub> support. Among the structural and textural properties, pore size is extremely essential because the diffusion of different species inside pores of Al<sub>2</sub>O<sub>3</sub> could affect and limit the HDS overall reaction rate. It is reported that the size of 4,6-DMDBT molecules estimated by molecular orbital calculations is 0.59 × 0.89 nm[22]. This pore size is favorable for the diffusion of the sulfur-containing alkyl derivatives of dibenzothiophene. Based on this mesoporous  $\gamma$ -Al<sub>2</sub>O<sub>3</sub> support, Co-Mo nanoparticles are deposited on support with the addition of the compound. To better show the role of the compound, Co-Mo/mesoporous  $\gamma$ -Al<sub>2</sub>O<sub>3</sub> catalyst without the addition of compound is compared. Fig. 2b shows the XRD patterns of Co-Mo/mesoporous  $\gamma$ -Al<sub>2</sub>O<sub>3</sub> and Co-Mo-C/mesoporous  $\gamma$ -Al<sub>2</sub>O<sub>3</sub> catalyst. Both of the two samples exhibit intense peaks at 46° and 66.8°, which are correlated to the planes (100) and (110) of the  $\gamma$ -Al<sub>2</sub>O<sub>3</sub> phase (JCPDF#29-0063)[23], respectively. There is no low-intensity broad peaks between 16° and 32°, indicating the absence of amorphous Al<sub>2</sub>O<sub>3</sub> phase. For Co-Mo/mesoporous  $\gamma$ -Al<sub>2</sub>O<sub>3</sub> catalyst, there is a peak at 26° which is related to the MoO<sub>3</sub> (021) species. In comparison, no peak shows up at 26° for Co-Mo-C/mesoporous  $\gamma$ -Al<sub>2</sub>O<sub>3</sub> catalyst, indicating that the particles are well-dispersed on support.

(Figure 2 should be inserted herein)

Acidity of a catalyst is a key parameter affecting the HDS performance[24]. For the mesoporous  $\gamma$ -Al<sub>2</sub>O<sub>3</sub> support, there are three kinds of NH<sub>3</sub>-TPD peaks corresponding to different strengths, i.e., weak acidity (150-250°C), medium acidity (250-450°C) and strong acidity (>450°C) [25, 26]. The total acid content includes 36.0% weak acidity,

1 64.0% medium acidity and 0% strong acidity. The total acid content of mesoporous  $\gamma$ -  
2  $\text{Al}_2\text{O}_3$  support is 0.654 mmol/g. After loading CoMo nanoparticles, the Lewis and  
3  
4 Brønsted sites of the two catalysts are determined by Py-IR. The bands at 1445 and  
5  
6 1556  $\text{cm}^{-1}$  are attributed to the pyridine chemisorbed on Lewis sites and the vibration  
7  
8 mode of pyridinium ion adsorbed on Brønsted sites, respectively[27]. In addition, the  
9  
10 pyridine adsorbed on both Lewis and Brønsted sites show up at 1486  $\text{cm}^{-1}$ . The  
11  
12 numbers of sites and B/L ratio of the two catalysts are listed in Table 1. It can be seen  
13  
14 from Table 1 that total acid sites together with B/L ratio are all larger on Co-Mo-  
15  
16 C/mesoporous  $\gamma$ - $\text{Al}_2\text{O}_3$  than those on Co-Mo/mesoporous  $\gamma$ - $\text{Al}_2\text{O}_3$  catalyst, possibly due  
17  
18 to the formation of complex between metal and multi-hydroxyl compound. This could  
19  
20 greatly affect the HDS reaction. It is reported that higher total acidity with larger B/L  
21  
22 ratio could enhance the HDS performance [28]. Therefore, the Co-Mo-C/mesoporous  $\gamma$ -  
23  
24  $\text{Al}_2\text{O}_3$  catalyst is expected to show better HDS activity.

25  
26  
27  
28  
29  
30  
31  
32  
33 (Table 1 should be inserted herein)

34  
35  
36 The interaction between metal and support is then investigated by  $\text{H}_2$ -TPR, which is a  
37  
38 powerful technique to investigate the reduction behavior of supported phases. Fig. 3  
39  
40 shows the  $\text{H}_2$ -TPR spectra of Co-Mo/mesoporous  $\gamma$ - $\text{Al}_2\text{O}_3$  and Co-Mo-C/mesoporous  $\gamma$ -  
41  
42  $\text{Al}_2\text{O}_3$  catalysts. According to Moulijn et al.[29], there is a reduction peak of well-  
43  
44 dispersed molybdenum supported species at low temperature of ca. 450°C. This is  
45  
46 attributed to the partial reduction of Mo(VI) to Mo(IV) of amorphous, highly defective,  
47  
48 multilayered oxides (octahedral Mo species) bounded to  $\text{Al}_2\text{O}_3$  support[30, 31]. It is  
49  
50 clear that the intense peak for Co-Mo-C/mesoporous  $\gamma$ - $\text{Al}_2\text{O}_3$  catalyst is located at  
51  
52 445°C, which is lower than 462.7°C for Co-Mo/mesoporous  $\gamma$ - $\text{Al}_2\text{O}_3$  catalyst,  
53  
54 demonstrating that the interaction between metal and support is weak for Co-Mo-  
55  
56  
57  
58  
59  
60  
61  
62  
63  
64  
65

1 C/mesoporous  $\gamma$ -Al<sub>2</sub>O<sub>3</sub> catalyst. This weak interaction is reported to be beneficial to the  
2 catalytic performance of HDS reaction due to the formation of Co-Mo-S type II sites[2].  
3  
4 Moreover, the absence of additional reduction peaks at 350 °C indicate that Co oxide  
5 supported crystallites is not formed on the supports.  
6  
7

8  
9  
10 (Figure 3 should be inserted herein)  
11

12  
13  
14 To obtain information regarding the morphology and distribution of Co-Mo-S  
15 **crystallites**, the two catalysts are then analyzed by HRTEM, and the typical HRTEM  
16 images are shown in Fig. 4. Due to the good dispersion of Co, the Co nanoparticles can  
17 not be observed by HRTEM characterization[32]. This is also in accordance with the  
18 XRD results in Fig. 2b. The black thread-like fringes are the Co-Mo-S phase. The  
19 average Co-Mo-S slab length (L) can be calculated from the following equation (3-1):  
20  
21  
22  
23  
24  
25  
26  
27  
28  
29  
30

$$\bar{L} = \frac{\sum_{i=1}^n n_i l_i}{\sum_{i=1}^n n_i} \quad (3-1)$$

31  
32  
33  
34  
35  
36  
37  
38 where  $l_i$  is the length of  $i$ th slab,  $n_i$  is the number of particle with a  $l_i$  length. The  
39 statistical results of the length and stacking distributions of Co-Mo-S for the two  
40 catalysts are shown in Table 2. Maximum slab length of Co-Mo-C/mesoporous  $\gamma$ -Al<sub>2</sub>O<sub>3</sub>  
41 catalyst is smaller, and the average length of the slabs on Co-Mo-C/mesoporous  $\gamma$ -  
42 Al<sub>2</sub>O<sub>3</sub> catalyst is 4.8 nm, shorter than the 9.5 nm for Co-Mo/mesoporous  $\gamma$ -Al<sub>2</sub>O<sub>3</sub>  
43 catalyst. In addition, the percentages of Co-Mo-S slabs with 1-2 layers are 75.2 and 47.9%  
44 for Co-Mo/mesoporous  $\gamma$ -Al<sub>2</sub>O<sub>3</sub> and Co-Mo-C/mesoporous  $\gamma$ -Al<sub>2</sub>O<sub>3</sub> catalysts,  
45 respectively. The percentages of 3-5 layers of Co-Mo/mesoporous  $\gamma$ -Al<sub>2</sub>O<sub>3</sub> and Co-Mo-  
46 C/mesoporous  $\gamma$ -Al<sub>2</sub>O<sub>3</sub> catalysts are 20.1 and 49.7%, respectively. **The results show that**  
47 **the addition of compound decrease the interaction between metal and support. Therefore,**  
48  
49  
50  
51  
52  
53  
54  
55  
56  
57  
58  
59  
60  
61  
62  
63  
64  
65

1 the average length reduces and the dispersion increases. Moreover, it is reported that the  
2 phase with 3-5 layers is Co-Mo-S type II, which could exhibit superior HDS  
3 performance than Co-Mo-S type I (1-2 layers)[33].  
4  
5  
6

7  
8 (Figure 4 should be inserted herein)  
9

10  
11 (Table 2 should be inserted herein)  
12  
13

14  
15 The surface concentrations of Mo in multiple oxidation states, and the binding  
16 energies of Co and Mo can be determined by XPS, as shown in Table 3. The catalysts  
17 are stored in nitrogen before XPS test to prevent the re-oxidation by air. The typical  
18 curve-fitting of Mo 3d is shown in Fig. S1. The Mo 3d spectra can be divided into three  
19 sets of doublets, which correspond to the Mo<sup>4+</sup>, Mo<sup>5+</sup> and Mo<sup>6+</sup> species[2]. The Mo<sup>4+</sup>  
20 species is usually MoS<sub>2</sub>, which is usually regarded as the active phase[28]. The Mo<sup>5+</sup>  
21 and Mo<sup>6+</sup> species can be attributed to Mo oxy-sulfide and not completely sulfided Mo  
22 species, respectively. From Fig. S1 and Table 3, it is seen that the percentage of Mo<sup>4+</sup> in  
23 the sum of Mo<sup>4+</sup>, Mo<sup>5+</sup> and Mo<sup>6+</sup> species is 75.03% for Co-Mo-C/mesoporous  $\gamma$ -Al<sub>2</sub>O<sub>3</sub>.  
24  
25 In comparison, this value for Co-Mo/mesoporous  $\gamma$ -Al<sub>2</sub>O<sub>3</sub> catalyst is only 65.88%. In  
26 addition, it is also noticed that the Mo binding energy for Co-Mo-C/mesoporous  $\gamma$ -  
27 Al<sub>2</sub>O<sub>3</sub> catalyst is also lower than that for Co-Mo/mesoporous  $\gamma$ -Al<sub>2</sub>O<sub>3</sub> catalyst. The  
28 lower binding energy and higher percentage of Mo<sup>4+</sup> all suggest that the Co-Mo-  
29 C/mesoporous  $\gamma$ -Al<sub>2</sub>O<sub>3</sub> catalyst has weaker interaction between metal and support, and  
30 thus is more easily sulfided, leading to more Co-Mo-S active phases. This finding is  
31 also in accordance with the finding of H<sub>2</sub>-TPR (Fig. 3) and HRTEM (Fig. 4) results.  
32  
33  
34  
35  
36  
37  
38  
39  
40  
41  
42  
43  
44  
45  
46  
47  
48  
49  
50  
51  
52  
53

54  
55 (Table 3 should be inserted herein)  
56  
57

### 58 **3.2 Catalytic performance of Co-Mo-C/mesoporous Al<sub>2</sub>O<sub>3</sub> catalyst**

59  
60  
61  
62  
63  
64  
65

1 The Co-Mo/mesoporous  $\gamma$ -Al<sub>2</sub>O<sub>3</sub> and Co-Mo-C/mesoporous  $\gamma$ -Al<sub>2</sub>O<sub>3</sub> catalysts are  
2 then tested for HDS reaction. The properties of the testing diesel oil are shown in Table  
3  
4 4. The sulfur content for this diesel oil is 9000  $\mu\text{g}\cdot\text{g}^{-1}$ . From table 4, it is seen the diesel  
5 has high sulfur and low nitrogen content, high 95% and FBP, indicating the difficulty of  
6  
7 HDS. The HDS results at different temperature for Co-Mo/mesoporous  $\gamma$ -Al<sub>2</sub>O<sub>3</sub> and Co-  
8  
9 Mo-C/mesoporous  $\gamma$ -Al<sub>2</sub>O<sub>3</sub> catalysts are summarized in Table 5. At 360°C, 6.0 MPa (H<sub>2</sub>  
10  
11 pressure) and 0.77 h<sup>-1</sup>, Co-Mo/mesoporous  $\gamma$ -Al<sub>2</sub>O<sub>3</sub> catalyst shows poor HDS  
12  
13 performance with the product sulfur content of 12  $\mu\text{g}\cdot\text{g}^{-1}$ . In contrast, the Co-Mo-  
14  
15 C/mesoporous  $\gamma$ -Al<sub>2</sub>O<sub>3</sub> catalyst has better performance. The low sulfur content of 7.4  
16  
17  $\mu\text{g}\cdot\text{g}^{-1}$  meets the requirement of Euro V standard. Further increasing the reaction  
18  
19 temperature leads to reduced sulfur contents. The values for Co-Mo/mesoporous  $\gamma$ -  
20  
21 Al<sub>2</sub>O<sub>3</sub> and Co-Mo-C/mesoporous  $\gamma$ -Al<sub>2</sub>O<sub>3</sub> catalysts are 7.0 and 4.0  $\mu\text{g}\cdot\text{g}^{-1}$ , respectively.  
22  
23 Therefore, the temperature for Co-Mo-C/mesoporous  $\gamma$ -Al<sub>2</sub>O<sub>3</sub> catalyst could be 10°C  
24  
25 lower than that for Co-Mo/mesoporous  $\gamma$ -Al<sub>2</sub>O<sub>3</sub> catalyst, which could greatly reduce the  
26  
27 energy consumption.  
28  
29  
30  
31  
32  
33  
34  
35

36 (Table 4 should be inserted herein)

37 (Table 5 should be inserted herein)

38  
39  
40  
41  
42 From the above results, the main reasons for the enhanced performance for Co-Mo-  
43  
44 C/mesoporous  $\gamma$ -Al<sub>2</sub>O<sub>3</sub> support could be the more active Co-Mo-S type II species,  
45  
46 which are originated from weak interaction between metal and support. The higher  
47  
48 activity of Co-Mo-S Type II is generally associated to the high stacking number of slabs  
49  
50 bonding weakly to the support through a small Mo-O-Al linkage[34]. Moreover, it is  
51  
52 also reported that the normal HDS reaction routes[28] include hydrogenation, direct  
53  
54 hydrogenolysis and alkyl transfer desulfurization. Higher B/L ratio and presence of Co-  
55  
56 Mo-S type II species may also lead to better alkyl transfer desulfurization of refractory  
57  
58  
59  
60  
61  
62  
63  
64  
65



1 sulfides such as 4, 6-DMDBT[23, 28]. The ultradeep hydrodesulfurization performance  
2 of Co-Mo-C/mesoporous  $\gamma$ -Al<sub>2</sub>O<sub>3</sub> catalyst is compared with reported catalysts. It can be  
3  
4 seen in Table 6 that the Co-Mo-C/mesoporous  $\gamma$ -Al<sub>2</sub>O<sub>3</sub> catalyst shows a high activity  
5 compared to catalysts reported in the literature[10, 34-38].  
6  
7

8  
9  
10  
11 (Table 6 should be inserted herein)  
12

13  
14 It has been confirmed that Co-Mo-C/mesoporous  $\gamma$ -Al<sub>2</sub>O<sub>3</sub> catalyst has enhanced  
15 performance for HDS reaction. To further verify the stability of this catalyst, the long-  
16 term stability is subsequently evaluated in industrial-scale 3000kt/a plant. The reaction  
17 conditions and results are shown in Table 7 and Fig. 5. The HDS reaction works at low  
18 H<sub>2</sub> pressure P=5.9 MPa, inlet temperature T<sub>i</sub>=350°C, outlet temperature T<sub>o</sub>=362°C,  
19 average temperature T<sub>a</sub>=358°C, hydrogen to oil ratio=308 and space velocity V=0.70h<sup>-1</sup>.  
20  
21 Clearly, the industrial evaluation of Co-Mo-C/mesoporous  $\gamma$ -Al<sub>2</sub>O<sub>3</sub> catalyst also meets  
22 the Euro V requirement of diesel with low sulfur content of 7.8  $\mu\text{g}\cdot\text{g}^{-1}$ . The long-term  
23 evaluation of catalyst at the same reaction condition is shown in Fig. 5. The catalyst  
24 maintains high stability with the low product sulfur content (i.e., smaller than 10  $\mu\text{g}\cdot\text{g}^{-1}$ )  
25 over 5000 h. The reason for the good catalytic stability should be the enhanced mass  
26 transfer ability together with the unique structure of active Co-Mo-S sites.  
27  
28  
29  
30  
31  
32  
33  
34  
35  
36  
37  
38  
39  
40  
41  
42  
43  
44

45 (Table 7 should be inserted herein)  
46

47  
48 (Figure 5 should be inserted herein)  
49

50  
51 It should be noted that the coke formation on Co-Mo-C/mesoporous  $\gamma$ -Al<sub>2</sub>O<sub>3</sub>  
52 catalyst is inevitable due to the contact with carbonaceous feedstock during the long-  
53 term stability test. Therefore, the reaction temperature is normally increased by ca.  
54 0.5°C/month to maintain the quality of products. After long running time, the catalyst  
55  
56  
57  
58  
59  
60  
61  
62  
63  
64  
65

1 should be regenerated. The fresh, used and regenerated catalysts in air at 420°C are then  
2 characterized by N<sub>2</sub> physisorption. Fig. 6 shows that all of the three samples show  
3 similar type IV adsorption-desorption isotherms. The hysteresis loop of the isotherm for  
4 the samples all start at ca. 0.4, indicating that the mesoporous structure is well  
5 maintained. The pore volume of the fresh catalyst is 0.33 cm<sup>3</sup>/g, which decreases to  
6 0.19 cm<sup>3</sup>/g after long-term testing. The regeneration successfully removes the  
7 carbonaceous deposits inside the pores, and increases the pore volume from 0.19 cm<sup>3</sup>/g  
8 to 0.33 cm<sup>3</sup>/g, which is almost the same to fresh catalyst. By using this catalyst, the  
9 3000 kt/a industrial plant in China with the catalyst technique from SINOPEC has been  
10 running smoothly for 3 years. After 3 years, the regenerated catalyst also shows good  
11 HDS performance (Table S2-3). This Co-Mo-C/mesoporous  $\gamma$ -Al<sub>2</sub>O<sub>3</sub> catalyst shows  
12 good performance with the reduced reaction temperature, saving the energy  
13 consumption and greatly increasing the profit. This catalyst is also of referential  
14 importance to the design of industrial catalyst for diesel ultra-deep hydrodesulfurization.  
15  
16  
17  
18  
19  
20  
21  
22  
23  
24  
25  
26  
27  
28  
29  
30  
31  
32

33 (Figure 6 should be inserted herein)  
34  
35  
36  
37

## 38 **4. Conclusion**

39  
40

41 In this work, hydrodesulfurization reaction catalyzed by Co-Mo-C/mesoporous  $\gamma$ -  
42 Al<sub>2</sub>O<sub>3</sub> catalyst at 3000 kt/a industrial-scale is investigated. The sulfur content can be  
43 reduced from 9000 to less than 10  $\mu$ g/g at 5.9MPa (H<sub>2</sub> pressure) and 358°C, meeting the  
44 requirement of Euro V standard. The Co-Mo-C/mesoporous  $\gamma$ -Al<sub>2</sub>O<sub>3</sub> catalyst can even  
45 show 5000 h long-term stability. This performance is much better than Co-  
46 Mo/mesoporous  $\gamma$ -Al<sub>2</sub>O<sub>3</sub> catalyst because the mesoporous  $\gamma$ -Al<sub>2</sub>O<sub>3</sub> support with pore  
47 diameter of 7.8 could facilitates the removal of large sulfide with diffusion limitation  
48 inside the limited pores. In addition, the addition of organic compound leads to  
49  
50  
51  
52  
53  
54  
55  
56  
57  
58  
59  
60  
61  
62  
63  
64  
65

1  
2  
3  
4  
5  
6  
7  
8  
9  
10  
11  
12  
13  
14  
15  
16  
17  
18  
19  
20  
21  
22  
23  
24  
25  
26  
27  
28  
29  
30  
31  
32  
33  
34  
35  
36  
37  
38  
39  
40  
41  
42  
43  
44  
45  
46  
47  
48  
49  
50  
51  
52  
53  
54  
55  
56  
57  
58  
59  
60  
61  
62  
63  
64  
65

increased acidity and weaker metal-support interaction. This enhances the sulfuration and generates more type II Co-Mo-S active phase. Moreover, the accumulation of coke during the reaction leads to the reduction of pore volume. Nevertheless, the coke be effectively removed by regeneration. The results are of essential reference to the design and development of HDS catalysts.

## References

- [1] A. A. Asadi, S. M. Alavi, S. J. Royae, M. Bazmi, Ultra-deep hydrodesulfurization of feedstock containing cracked gasoil through NiMo/ $\gamma$ -Al<sub>2</sub>O<sub>3</sub> catalyst pore size optimization, *Energy Fuels* 32 (2018) 2203-2212.
- [2] F. Rashidi, T. Sasaki, A. M. Rashidi, A. N. Kharat, K. J. Jozani, Ultradeep hydrodesulfurization of diesel fuels using highly efficient nanoalumina-supported catalysts: Impact of support, phosphorus, and/or boron on the structure and catalytic activity, *J. Catal.* 299 (2013) 321-335.
- [3] P. A. Nikulshin, A. V. Mozhaev, A. A. Pimerzin, V. V. Kononov, A. A. Pimerzin, CoMo/Al<sub>2</sub>O<sub>3</sub> catalysts prepared on the basis of Co<sub>2</sub>Mo<sub>10</sub>-heteropolyacid and cobalt citrate: Effect of Co/Mo ratio, *Fuel* 100 (2012) 24-33.
- [4] Y. Chen, H. Song, H. Meng, Y. Lu, C. Li, Z. G. Lei, Polyethylene glycol oligomers as green and efficient extractant for extractive catalytic oxidative desulfurization of diesel. *Fuel Process. Tech.*, 158 (2017) 20-25.
- [5] J. V. Lauritsen, F. Besenbacher, Atom-resolved scanning tunneling microscopy investigations of molecular adsorption on MoS<sub>2</sub> and CoMoS hydrodesulfurization catalysts, *J. Catal.* 328 (2015) 49-58.
- [6] L. van Haandel, G. Bremmer, E. Hensen, T. Weber, Influence of sulfiding agent and pressure on structure and performance of CoMo/Al<sub>2</sub>O<sub>3</sub> hydrodesulfurization catalysts, *J. Catal.* 342 (2016) 27-39.
- [7] Q. Sheng, G. Wang, Y. J. Liu, M. M. Husein, C.D. Gao, Q. Shi, J. S. Gao. Combined Hydrotreating and Fluid Catalytic Cracking Processing for the Conversion of Inferior Coker Gas Oil: Effect on Nitrogen Compounds and Condensed Aromatics. *Energy Fuels* 32(2018) 4979-4987.
- [8] T. Fujikawa, H. Kimura, K. Kiriyama, K. Hagiwara, Development of ultra-deep HDS catalyst for

1 production of clean diesel fuels, *Catal. Today* 111 (2006) 188-193.

2 [9] M.H. Zhang, J.Y. Fan, K. Chi, A. J. Duan, Z. Zhao, X.L. Meng, et al., Synthesis, characterization,  
3 and catalytic performance of NiMo catalysts supported on different crystal alumina materials in the  
4 hydrodesulfurization of diesel, *Fuel Process. Tech.* 156 (2017) 446-453.

5 [10] Y. J. Liu, S. Z. Song, X. Deng, W. Huang, Diesel Ultradeep Hydrodesulfurization over  
6 Trimetallic WMoNi Catalysts by a Liquid-Phase Preparation Method in a Slurry Bed Reactor,  
7 *Energy Fuels* 31 (2017) 7372-7381.

8 [11] T. C. Ho, A theory of ultradeep hydrodesulfurization of diesel in stacked-bed reactors, *AIChE J.*  
9 64 (2018) 595-605.

10 [12] W. Chen, X. Long, M. Li, H. Nie, D. Li, Influence of active phase structure of CoMo/Al<sub>2</sub>O<sub>3</sub>  
11 catalyst on the selectivity of hydrodesulfurization and hydrodearomatization, *Catal. Today* 292 (2017)  
12 97-109.

13 [13] S. Boonyasuwat, J. Tscheikuna, Co-processing of palm fatty acid distillate and light gas oil in  
14 pilot-scale hydrodesulfurization unit over commercial CoMo/Al<sub>2</sub>O<sub>3</sub>, *Fuel* 199 (2017) 115-124.

15 [14] O. Klimov, K. Nadeina, Y. V. Vatutina, E. Stolyarova, I. Danilova, E. Y. Gerasimov, et al.,  
16 CoMo/Al<sub>2</sub>O<sub>3</sub> hydrotreating catalysts of diesel fuel with improved hydrodenitrogenation activity,  
17 *Catal. Today* 307(2018)73-83.

18 [15] J. V. Lauritsen, J. Kibsgaard, G. H. Olesen, P. G. Moses, B. Hinnemann, S. Helveg, et al.,  
19 Location and coordination of promoter atoms in Co-and Ni-promoted MoS<sub>2</sub>-based hydrotreating  
20 catalysts, *J. Catal.* 249 (2007) 220-233.

21 [16] J. Chen, J. Mi, K. Li, X. Wang, E. Dominguez Garcia, Y. Cao, et al., Role of Citric Acid in  
22 Preparing Highly Active CoMo/Al<sub>2</sub>O<sub>3</sub> Catalyst: From Aqueous Impregnation Solution to Active Site  
23 Formation, *Ind. Eng. Chem. Res.* 56 (2017) 14172-14181.

24 [17] G. M. Dhar, B. Srinivas, M. Rana, M. Kumar, S. Maity, Mixed oxide supported  
25 hydrodesulfurization catalysts-a review, *Catal. Today* 86 (2003) 45-60.

26 [18] R. Huirache-Acuña, B. Pawelec, E. Rivera-Muñoz, R. Guil-López, J. Fierro, Characterization  
27 and HDS activity of sulfided CoMoW/SBA-16 catalysts: Effects of P addition and Mo/(Mo+ W)  
28 ratio, *Fuel* 198 (2017) 145-158.

29 [19] R. Nava, A. Infantes-Molina, P. Castaño, R. Guil-López, B. Pawelec, Inhibition of CoMo/HMS  
30  
31  
32  
33  
34  
35  
36  
37  
38  
39  
40  
41  
42  
43  
44  
45  
46  
47  
48  
49  
50  
51  
52  
53  
54  
55  
56  
57  
58  
59  
60  
61  
62  
63  
64  
65

1 catalyst deactivation in the HDS of 4, 6-DMDBT by support modification with phosphate, Fuel 90  
2 (2011) 2726-2737.

3  
4 [20] S. A. Ali, S. Ahmed, K. W. Ahmed, M. A. Al-Saleh, Simultaneous hydrodesulfurization of  
5 dibenzothiophene and substituted dibenzothiophenes over phosphorus modified CoMo/Al<sub>2</sub>O<sub>3</sub>  
6 catalysts, Fuel Process. Tech. 98 (2012) 39-44.

7  
8  
9  
10 [21] X. Feng, J. Yang, X.Z. Duan, Y.Q. Cao, B.X. Chen, W.Y. Chen, D. Lin, G. Qian, D. Chen, C.H.  
11 Yang, X.G. Zhou, Enhanced catalytic performance for propene epoxidation with H<sub>2</sub> and O<sub>2</sub> over  
12 bimetallic Au-Ag/Uncalcined TS-1 catalysts, ACS Catal. 8 (2018) 7799–7808.

13  
14  
15  
16 [22] K. S. Triantafyllidis, E. A. Deliyanni, Desulfurization of diesel fuels: Adsorption of 4,6-  
17 DMDBT on different origin and surface chemistry nanoporous activated carbons, Chem. Eng. J. 236  
18 (2014) 406-414.

19  
20  
21 [23] C. Peng, R. Guo, X.C. Fang, Improving ultra-deep desulfurization efficiency by catalyst  
22 stacking technology, Catal. Lett. 146 (2016) 701-709.

23  
24  
25 [24] V. Sundaramurthy, A. Dalai, J. Adjaye, The effect of phosphorus on hydrotreating property of  
26 NiMo/γ-Al<sub>2</sub>O<sub>3</sub> nitride catalyst, Appl. Catal. A: Gen. 335 (2008) 204-210.

27  
28  
29 [25] B. Pawelec, J. Fierro, A. Montesinos, T. Zepeda, Influence of the acidity of nanostructured  
30 CoMo/P/Ti-HMS catalysts on the HDS of 4, 6-DMDBT reaction pathways, Appl. Catal. B: Environ.  
31 80 (2008) 1-14.

32  
33  
34 [26] J. D. de León, T. Zepeda, G. Alonso-Nuñez, D. Galván, B. Pawelec, S. Fuentes, Insight of 1D γ-  
35 Al<sub>2</sub>O<sub>3</sub> nanorods decoration by NiWS nanoslabs in ultra-deep hydrodesulfurization catalyst, J. Catal.  
36 321 (2015) 51-61.

37  
38  
39 [27] C. Kwak, J. J. Lee, J. S. Bae, S. H. Moon, Poisoning effect of nitrogen compounds on the  
40 performance of CoMoS/Al<sub>2</sub>O<sub>3</sub> catalyst in the hydrodesulfurization of dibenzothiophene, 4-  
41 methylthiobenzothiophene, and 4, 6-dimethylthiobenzothiophene, Appl. Catal. B: Environ. 35 (2001)  
42 59-68.

43  
44  
45 [28] X. C. Fang, R. Guo, et al., The development and application of catalysts for ultra-deep  
46 hydrodesulfurization of diesel, Chin. J. Catal. 34 (2013) 130-139.

47  
48  
49 [29] P. Arnoldy, M. Franken, B. Scheffer, J. Moulijn, Temperature-programmed reduction of  
50 CoOMoO<sub>3</sub>Al<sub>2</sub>O<sub>3</sub> catalysts, J. Catal. 96 (1985) 381-395.

51  
52  
53  
54  
55  
56  
57  
58  
59  
60  
61  
62  
63  
64  
65

- 1  
2  
3  
4  
5  
6  
7  
8  
9  
10  
11  
12  
13  
14  
15  
16  
17  
18  
19  
20  
21  
22  
23  
24  
25  
26  
27  
28  
29  
30  
31  
32  
33  
34  
35  
36  
37  
38  
39  
40  
41  
42  
43  
44  
45  
46  
47  
48  
49  
50  
51  
52  
53  
54  
55  
56  
57  
58  
59  
60  
61  
62  
63  
64  
65
- [30] E. Rodríguez-Castellón, A. Jiménez-López, D. Eliche-Quesada, Nickel and cobalt promoted tungsten and molybdenum sulfide mesoporous catalysts for hydrodesulfurization, *Fuel* 87 (2008) 1195-1206.
- [31] L. Pena, D. Valencia, T. Klimova, CoMo/SBA-15 catalysts prepared with EDTA and citric acid and their performance in hydrodesulfurization of dibenzothiophene, *Appl. Catal. B: Environ.* 147 (2014) 879-887.
- [32] S. Eijsbouts, L. Van den Oetelaar, R. Van Puijenbroek, MoS<sub>2</sub> morphology and promoter segregation in commercial Type 2 Ni-Mo/Al<sub>2</sub>O<sub>3</sub> and Co-Mo/Al<sub>2</sub>O<sub>3</sub> hydroprocessing catalysts, *J. Catal.* 229 (2005) 352-364.
- [33] K. Xu, Y. Li, X. Xu, C. Zhou, Z. Liu, F. Yang, et al., Single-walled carbon nanotubes supported Ni-Y as catalyst for ultra-deep hydrodesulfurization of gasoline and diesel, *Fuel* 160 (2015) 291-296.
- [34] F. Rashidi, T. Sasaki, A. M. Rashidi, A. Nemat Kharat, K. J. Jozani, Ultradeep hydrodesulfurization of diesel fuels using highly efficient nanoalumina-supported catalysts: Impact of support, phosphorus, and/or boron on the structure and catalytic activity, *J. Catal.* 299 (2013) 321-335.
- [35] W. Zhou, Q. Zhang, Y. Zhou, Q. Wei, L. Du, S. Ding, et al., Effects of Ga- and P-modified USY-based NiMoS catalysts on ultra-deep hydrodesulfurization for FCC diesels, *Catal. Today* 305 (2018) 171-181.
- [36] S. Shan, H. Liu, Y. Yue, G. Shi, X. Bao, Trimetallic WMoNi diesel ultra-deep hydrodesulfurization catalysts with enhanced synergism prepared from inorganic-organic hybrid nanocrystals, *J. Catal.* 344 (2016) 325-333.
- [37] L. Peña, D. Valencia, T. Klimova, CoMo/SBA-15 catalysts prepared with EDTA and citric acid and their performance in hydrodesulfurization of dibenzothiophene, *Appl. Catal. B: Environ.* 147 (2014) 879-887.
- [38] T. Kabe, W. H. Qian, S. Ogawa, A. Ishihara, Mechanism of Hydrodesulfurization of Dibenzothiophene on Co-Mo/Al<sub>2</sub>O<sub>3</sub> and Co/Al<sub>2</sub>O<sub>3</sub> Catalyst by the Use of Radioisotope <sup>35</sup>S Tracer, *J. Catal.* 143 (1993) 239-248.

**Table Captions:**

**Table 1** Acidity for Co-Mo/mesoporous  $\gamma$ -Al<sub>2</sub>O<sub>3</sub> and Co-Mo-C/mesoporous  $\gamma$ -Al<sub>2</sub>O<sub>3</sub> catalyst.

**Table 2** HRTEM statistic results of Co-Mo/mesoporous  $\gamma$ -Al<sub>2</sub>O<sub>3</sub> and Co-Mo-C/mesoporous  $\gamma$ -Al<sub>2</sub>O<sub>3</sub> catalyst.

**Table 3** XPS results of sulfurized Co-Mo/mesoporous  $\gamma$ -Al<sub>2</sub>O<sub>3</sub> and Co-Mo-C/mesoporous  $\gamma$ -Al<sub>2</sub>O<sub>3</sub> catalysts.

**Table 4** Properties of testing feedstocks for HDS reaction.

**Table 5** Comparison of HDS results for different catalysts.

**Table 6** Comparing the catalytic activity of the Co-Mo-C/mesoporous  $\gamma$ -Al<sub>2</sub>O<sub>3</sub> catalyst and other reported catalysts.

**Table 7** Reaction conditions and results in hydrotreating unit.

1  
2  
3  
4  
5  
6  
7  
8  
9  
10  
11  
12  
13  
14  
15  
16  
17  
18  
19  
20  
21  
22  
23  
24  
25  
26  
27  
28  
29  
30  
31  
32  
33  
34  
35  
36  
37  
38  
39  
40  
41  
42  
43  
44  
45  
46  
47  
48  
49  
50  
51  
52  
53  
54  
55  
56  
57  
58  
59  
60  
61  
62  
63  
64  
65

**Table 1** Acidity for Co-Mo/mesoporous  $\gamma$ -Al<sub>2</sub>O<sub>3</sub> and Co-Mo-C/mesoporous  $\gamma$ -Al<sub>2</sub>O<sub>3</sub> catalyst.

Catalysts	Total acidity ( $\mu\text{mol/g}$ )	Brönsted ( $\mu\text{mol/g}$ )	Lewis ( $\mu\text{mol/g}$ )	B/L ratio
Co-Mo-C/mesoporous $\gamma$ - Al <sub>2</sub> O <sub>3</sub>	544	139	405	0.34
Co-Mo/mesoporous $\gamma$ - Al <sub>2</sub> O <sub>3</sub>	487	44	443	0.10

1  
2  
3  
4  
5  
6  
7  
8  
9  
10  
11  
12  
13  
14  
15  
16  
17  
18  
19  
20  
21  
22  
23  
24  
25  
26  
27  
28  
29  
30  
31  
32  
33  
34  
35  
36  
37  
38  
39  
40  
41  
42  
43  
44  
45  
46  
47  
48  
49  
50  
51  
52  
53  
54  
55  
56  
57  
58  
59  
60  
61  
62  
63  
64  
65



**Table 2** HRTEM statistic results of Co-Mo/mesoporous  $\gamma$ -Al<sub>2</sub>O<sub>3</sub> and Co-Mo-C/mesoporous  $\gamma$ -Al<sub>2</sub>O<sub>3</sub> catalyst.

Properties	Co-Mo/mesoporous	Co-Mo-C/mesoporous
	$\gamma$ -Al <sub>2</sub> O <sub>3</sub>	$\gamma$ -Al <sub>2</sub> O <sub>3</sub>
Maximum slab length (nm)	17.3	11.1
Average slab length (nm)	9.5	4.8
Percentage of 1-2 layers	75.2	47.9
Percentage of 3-5 layers	20.1	49.7
Percentage of >5 layers	4.7	2.4

1  
2  
3  
4  
5  
6  
7  
8  
9  
10  
11  
12  
13  
14  
15  
16  
17  
18  
19  
20  
21  
22  
23  
24  
25  
26  
27  
28  
29  
30  
31  
32  
33  
34  
35  
36  
37  
38  
39  
40  
41  
42  
43  
44  
45  
46  
47  
48  
49  
50  
51  
52  
53  
54  
55  
56  
57  
58  
59  
60  
61  
62  
63  
64  
65

**Table 3** XPS results of sulfurized Co-Mo/mesoporous  $\gamma$ -Al<sub>2</sub>O<sub>3</sub> and Co-Mo-C/mesoporous  $\gamma$ -Al<sub>2</sub>O<sub>3</sub> catalysts.

Catalyst	Co-Mo/mesoporous $\gamma$ -Al <sub>2</sub> O <sub>3</sub>	Co-Mo-C/mesoporous $\gamma$ -Al <sub>2</sub> O <sub>3</sub>
Mo <sup>4+</sup> /(Mo <sup>4+</sup> +Mo <sup>5+</sup> +Mo <sup>6+</sup> ) (%)	65.88	75.03
S/Mo	1.74	1.78
Mo 3d <sub>5/2</sub> BE (eV)	228.8	228.5
Co 2p <sub>3/2</sub> BE (eV)	780.1	778.4

1  
2  
3  
4  
5  
6  
7  
8  
9  
10  
11  
12  
13  
14  
15  
16  
17  
18  
19  
20  
21  
22  
23  
24  
25  
26  
27  
28  
29  
30  
31  
32  
33  
34  
35  
36  
37  
38  
39  
40  
41  
42  
43  
44  
45  
46  
47  
48  
49  
50  
51  
52  
53  
54  
55  
56  
57  
58  
59  
60  
61  
62  
63  
64  
65

**Table 4** Properties of testing feedstocks for HDS reaction.

Feedstock	Diesel oil
Density at 20°C (g/cm <sup>3</sup> )	0.8397
Distillation range (°C)	
IBP (10%)	151/189
30%/50%	242/286
70%/90%	312/352
95%/FBP	366/378
Sulfur content (μg·g <sup>-1</sup> )	9000
Nitrogen content (μg·g <sup>-1</sup> )	150
4,6-DMDBT content (μg·g <sup>-1</sup> )	192

1  
2  
3  
4  
5  
6  
7  
8  
9  
10  
11  
12  
13  
14  
15  
16  
17  
18  
19  
20  
21  
22  
23  
24  
25  
26  
27  
28  
29  
30  
31  
32  
33  
34  
35  
36  
37  
38  
39  
40  
41  
42  
43  
44  
45  
46  
47  
48  
49  
50  
51  
52  
53  
54  
55  
56  
57  
58  
59  
60  
61  
62  
63  
64  
65

**Table 5** Comparison of HDS results for different catalysts.

Feedstock	Diesel oil			
Catalyst	Co-Mo-C/mesoporous $\gamma$ - $\text{Al}_2\text{O}_3$	Co-Mo/mesoporous $\gamma$ - $\text{Al}_2\text{O}_3$		
HDS conditions				
Average reaction temperature ( $^{\circ}\text{C}$ )	360	370	360	370
Hydrogen pressure (MPa)	6.0	6.0	6.0	6.0
Space velocity ( $\text{h}^{-1}$ )	0.77	0.77	0.77	0.77
Hydrogen/oil ratio	400	400	400	400
Sulfur content ( $\mu\text{g}\cdot\text{g}^{-1}$ )	7.4	4.0	12.0	7.0
Nitrogen content ( $\mu\text{g}\cdot\text{g}^{-1}$ )	2.4	2.2	5.0	4.0
4,6-DMDBT content ( $\mu\text{g}\cdot\text{g}^{-1}$ )	4.2	2.5	8.2	4.6

**Table 6** Comparing the catalytic activity of the Co-Mo-C/mesoporous  $\gamma$ -Al<sub>2</sub>O<sub>3</sub> catalyst and other reported catalysts.

Catalysts	Sulfur Concentration (ppm)	Conversion (%)	Temperature(°C)	Stability (h)	Reference
Co-Mo-C/mesoporous $\gamma$ -Al <sub>2</sub> O <sub>3</sub>	9000	99.9	358	5000	This work
CoMoPB/nanoAl <sub>2</sub> O <sub>3</sub>	13500	99.9	350	-	[34]
PGaHUSY	2259	99.7	360	-	[38]
WMoNi-HHD	3904	99.5	360	500	[37]
WMoNi/Al <sub>2</sub> O <sub>3</sub>	-	96.0	360	-	[10]
CoMo/SBA-15	2160	77	3000	-	[36]
Co-Mo/Al <sub>2</sub> O <sub>3</sub>	4000	67	3000	-	[35]

1  
2  
3  
4  
5  
6  
7  
8  
9  
10  
11  
12  
13  
14  
15  
16  
17  
18  
19  
20  
21  
22  
23  
24  
25  
26  
27  
28  
29  
30  
31  
32  
33  
34  
35  
36  
37  
38  
39  
40  
41  
42  
43  
44  
45  
46  
47  
48  
49  
50  
51  
52  
53  
54  
55  
56  
57  
58  
59  
60  
61  
62  
63  
64  
65

**Table 7** Reaction conditions and results in hydrotreating unit.

Catalyst	Co-Mo-C/mesoporous $\gamma$ -Al <sub>2</sub> O <sub>3</sub>	
Diesel	Feedstock	Product
Density at 20°C (g/m <sup>3</sup> )	839.0	831.6
Distillation range (D86, °C)		
IBP/10%	158/191	175/198
30%/50%	233/275	232/274
70%/90	313/349	311/348
95%/FBP	363/367	362/365
Sulfur content ( $\mu\text{g}\cdot\text{g}^{-1}$ )	9000	7.8

**Figure Captions:**

**Fig. 1** Schematic process flow diagram of 3000 kt/a industrial-scale diesel ultra-deep hydrodesulfurization.

**Fig. 2** XRD patterns (a) of mesoporous  $\gamma$ - $\text{Al}_2\text{O}_3$  support and  $\text{N}_2$  physisorption (b) of catalysts.

**Fig. 3**  $\text{H}_2$ -TPR spectra of Co-Mo/mesoporous  $\gamma$ - $\text{Al}_2\text{O}_3$  and Co-Mo-C/mesoporous  $\gamma$ - $\text{Al}_2\text{O}_3$  catalyst.

**Fig. 4** Typical HRTEM of Co-Mo/mesoporous  $\gamma$ - $\text{Al}_2\text{O}_3$  (a) and Co-Mo-C/mesoporous  $\gamma$ - $\text{Al}_2\text{O}_3$  catalysts (b).

**Fig. 5** Industrial-scale 3000 kt/a stability evaluation (a) in a hydrotreating plant (b).

**Fig. 6**  $\text{N}_2$  adsorption-desorption isotherms of fresh, deactivated and regenerated Co-Mo-C/mesoporous  $\gamma$ - $\text{Al}_2\text{O}_3$  catalysts.

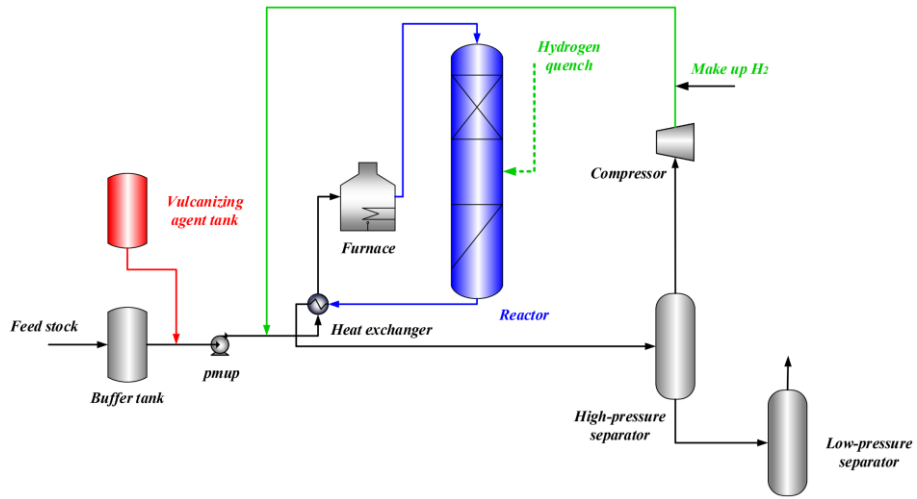


**Fig. 1** Schematic process flow diagram of 3000 kt/a industrial-scale diesel ultra-deep hydrodesulfurization.

1  
2  
3  
4  
5  
6  
7  
8  
9  
10  
11  
12  
13  
14  
15  
16  
17  
18  
19  
20  
21  
22  
23  
24  
25  
26  
27  
28  
29  
30  
31  
32  
33  
34  
35  
36  
37  
38  
39  
40  
41  
42  
43  
44  
45  
46  
47  
48  
49  
50  
51  
52  
53  
54  
55  
56  
57  
58  
59  
60  
61  
62  
63  
64  
65



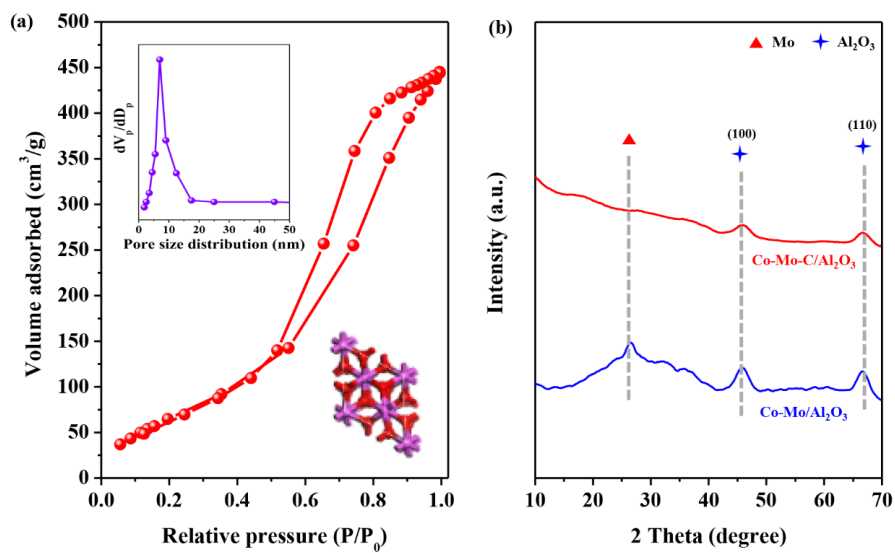


**Fig. 2** XRD patterns (a) of mesoporous  $\gamma$ - $\text{Al}_2\text{O}_3$  support and  $\text{N}_2$  physisorption (b) of catalysts.

1  
2  
3  
4  
5  
6  
7  
8  
9  
10  
11  
12  
13  
14  
15  
16  
17  
18  
19  
20  
21  
22  
23  
24  
25  
26  
27  
28  
29  
30  
31  
32  
33  
34  
35  
36  
37  
38  
39  
40  
41  
42  
43  
44  
45  
46  
47  
48  
49  
50  
51  
52  
53  
54  
55  
56  
57  
58  
59  
60  
61  
62  
63  
64  
65

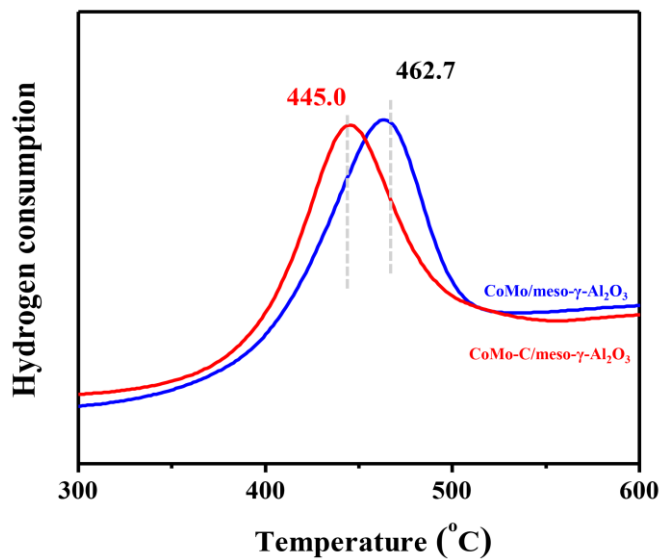


**Fig. 3** H<sub>2</sub>-TPR spectra of Co-Mo/mesoporous  $\gamma$ -Al<sub>2</sub>O<sub>3</sub> and Co-Mo-C/mesoporous  $\gamma$ -Al<sub>2</sub>O<sub>3</sub> catalyst.

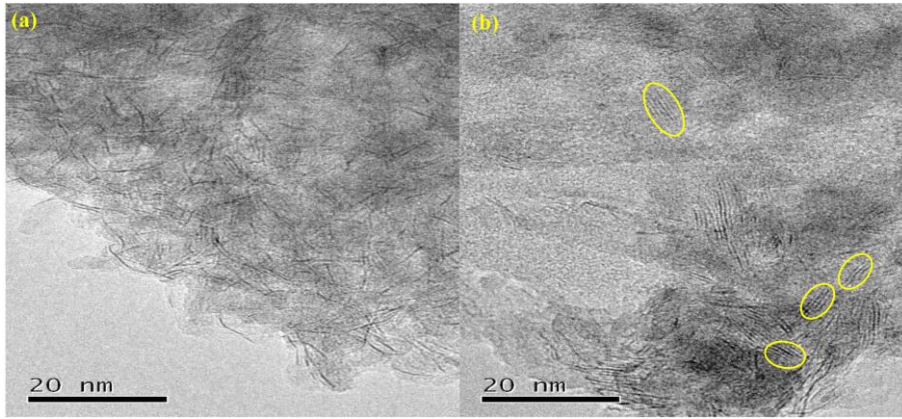


**Fig. 4** Typical HRTEM of Co-Mo/mesoporous  $\gamma$ -Al<sub>2</sub>O<sub>3</sub> (a) and Co-Mo-C/mesoporous  $\gamma$ -Al<sub>2</sub>O<sub>3</sub> catalysts (b).

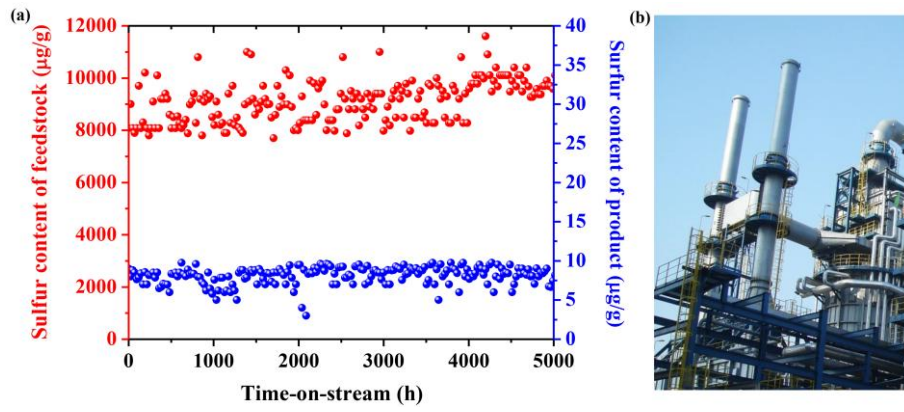


**Fig. 5** Industrial-scale 3000 kt/a stability evaluation (a) in a hydrotreating plant (b).

1  
2  
3  
4  
5  
6  
7  
8  
9  
10  
11  
12  
13  
14  
15  
16  
17  
18  
19  
20  
21  
22  
23  
24  
25  
26  
27  
28  
29  
30  
31  
32  
33  
34  
35  
36  
37  
38  
39  
40  
41  
42  
43  
44  
45  
46  
47  
48  
49  
50  
51  
52  
53  
54  
55  
56  
57  
58  
59  
60  
61  
62  
63  
64  
65

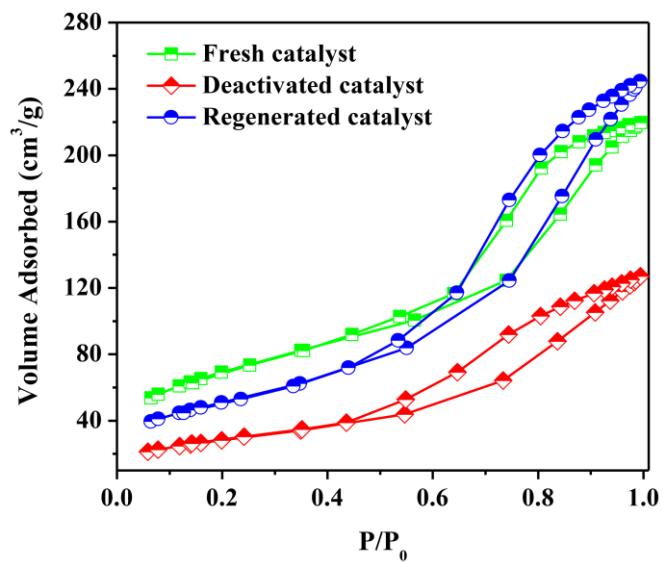


**Fig. 6** N<sub>2</sub> adsorption-desorption isotherms of fresh, deactivated and regenerated Co-Mo-C/mesoporous  $\gamma$ -Al<sub>2</sub>O<sub>3</sub> catalysts.

1  
2  
3  
4  
5  
6  
7  
8  
9  
10  
11  
12  
13  
14  
15  
16  
17  
18  
19  
20  
21  
22  
23  
24  
25  
26  
27  
28  
29  
30  
31  
32  
33  
34  
35  
36  
37  
38  
39  
40  
41  
42  
43  
44  
45  
46  
47  
48  
49  
50  
51  
52  
53  
54  
55  
56  
57  
58  
59  
60  
61  
62  
63  
64  
65

1  
2  
3  
4  
5  
6  
7  
8  
9  
10  
11  
12  
13  
14  
15  
16  
17  
18  
19  
20  
21  
22  
23  
24  
25  
26  
27  
28  
29  
30  
31  
32  
33  
34  
35  
36  
37  
38  
39  
40  
41  
42  
43  
44  
45  
46  
47  
48  
49  
50  
51  
52  
53  
54  
55  
56  
57  
58  
59  
60  
61  
62  
63  
64  
65

# Tailoring the structure of Co-Mo/mesoporous $\gamma$ -Al<sub>2</sub>O<sub>3</sub> catalysts by adding multi-hydroxyl compound: A 3000 kt/a industrial-scale diesel ultra-deep hydrodesulfurization study

Chong Peng<sup>†</sup>, Rong Guo<sup>†</sup>, Xiang Feng<sup>\*\*</sup> and Xiangchen Fang<sup>\*\*</sup>

<sup>†</sup> Dalian Research Institute of Petroleum and Petrochemicals, SINOPEC, Dalian 116045, China

<sup>\*\*</sup> State Key Laboratory of Heavy Oil Processing, China University of Petroleum, Qingdao 266580, China

**Abstract:** Ever-increasing concern on environmental impacts (e.g., sulfur pollution) by fossil fuels has triggered the research on hydrodesulfurization (HDS). In this work, Co-Mo nanoparticles were deposited on the mesoporous  $\gamma$ -Al<sub>2</sub>O<sub>3</sub> support with the addition of organic compound, and the physico-chemical properties of the catalysts (Co-Mo-C/mesoporous  $\gamma$ -Al<sub>2</sub>O<sub>3</sub>) were then characterized by multi-techniques such as H<sub>2</sub>-TPR, HRTEM, XPS, N<sub>2</sub> physisorption. It is found that the Co-Mo-C/mesoporous  $\gamma$ -Al<sub>2</sub>O<sub>3</sub> catalyst is easier to be reduced when organic compound is added, enhancing the sulfuration. This results in better dispersion of Co-Mo-S species and more Co-Mo-S II active sites, which significantly enhance diesel ultra-deep hydrodesulfurization activity. Furthermore, this novel catalyst was also tested for HDS reaction in a 3000 kt/a industrial-scale plant. Gratifyingly, this catalyst showed effective reduction of sulfur content from 9000 to less than 10  $\mu$ g/g and also high stability over 5000 h. The results are of great significance to the design and development of industrial HDS catalysts.

**Keywords:** hydrodesulfurization; diesel; structure manipulation; Co-Mo/mesoporous Al<sub>2</sub>O<sub>3</sub>; industrial-scale

# 1. Introduction

Growing concern on environment necessitates the elimination of heteroatoms such as sulfur and nitrogen from fossil fuels. This worldwide demand for clean fuels leads to strict legislation to control and decrease the environmental impacts of fossil fuels on the environment and human beings. For example, Euro V standard of diesel fuel strictly requires that the diesel sulfur content is less than 10 ppm[1]. However, the removal of refractive sulfur-containing alkyl derivatives of dibenzothiophene (DBTs)[2], such as 4-dimethyldibenzothiophene (4-MDBT) and 4,6-dimethyldibenzothiophene (4,6-DMDBT), is quite challenging. Ultra-deep hydrodesulfurization (HDS) to produce ultra-low-sulfur[3] diesel fuels with sulfur content of less than 10 ppm is one of the most essential industrial processes to resolve the above problem[4-6]. This has triggered the great attention of researchers on developing highly efficient catalysts for HDS [7-11].

The most important HDS catalyst used in oil refineries is usually the Co(Ni)Mo/Al<sub>2</sub>O<sub>3</sub> catalysts [12-14]. The structure of the typical Co(Ni)-Mo catalyst can be briefly described by the Co(Ni)-Mo-S model, which was first reported by Topsøe[15]. The structure of catalytically active Co(Ni)-Mo-S sites is formed by the decoration of Co(Ni) atoms on the well-dispersed MoS<sub>2</sub> nanocrystals[16]. These active sites can be obtained by the sulfidation process[3]. It is widely accepted that the HDS activity and stability of the catalysts are greatly affected by the physico-chemical properties of the support and metals [1, 2]. Al<sub>2</sub>O<sub>3</sub> in  $\alpha$  and  $\gamma$  forms is the most common support for HDS catalysts because of its outstanding textural and mechanical properties. Normally, these properties can be easily tuned based on the detailed reaction requirements, feedstock compositions and product's targeted specifications[17].

1  
2  
3  
4  
5  
6  
7  
8  
9  
10  
11  
12  
13  
14  
15  
16  
17  
18  
19  
20  
21  
22  
23  
24  
25  
26  
27  
28  
29  
30  
31  
32  
33  
34  
35  
36  
37  
38  
39  
40  
41  
42  
43  
44  
45  
46  
47  
48  
49  
50  
51  
52  
53  
54  
55  
56  
57  
58  
59  
60  
61  
62  
63  
64  
65

Besides the properties of support, the interaction between the support and Co-Mo metals are usually quite essential to the design of effective HDS catalyst. It was reported that using chelating agents or additives such as P and B can reduce the interaction between active metals and aluminum supports, producing more active HDS sites [18-20]. Although much attention has been devoted to understanding the effect of support properties on HDS performance, few reports were focused on enhancing catalytic performance by manipulating the metal-support interaction aiming at industrial application. There is urgent need to design suitable catalyst for industrial HDS reaction, which is of prime scientific and industrial importance.

In this work, the effects of organic compound on catalyst structure and HDS performance are investigated, aiming at the industrial-scale HDS process development. Mesoporous  $\gamma$ -Al<sub>2</sub>O<sub>3</sub> is first employed as support, and then load Co-Mo nanoparticles with the addition of organic compound. The physico-chemical properties of the catalysts are studied by multi-techniques such as XRD, XPS, TPR, HRTEM, NH<sub>3</sub>-TPD and Py-IR. It is found that the introduction of organic compound makes the catalyst easily reduced, generating more type II Co-Mo-S active sites and enhancing the HDS activity and stability. Moreover, this catalyst is also tested in an 3000 kt/a industrial-scale HDS unit, and shows fantastic 99.9% sulfur reduction from 9000 to less than 10  $\mu$ g/g over 5000 h. The properties of the used catalyst after long-term evaluation and regeneration are further discussed. The results reported herein are of great referential importance to the design of industrial catalysts, and is expected to be extended to other HDS catalysts.

## 2. Experimental

### 2.1 Synthesis of Co-Mo/mesoporous $\gamma$ -Al<sub>2</sub>O<sub>3</sub> catalyst

The mesoporous  $\gamma$ -Al<sub>2</sub>O<sub>3</sub> support was provided by Fushun Catalysts Factory of



1 SINOPEC. Two Co-Mo catalysts were prepared by impregnation with an aqueous  
2 solution of cobalt nitrate  $[\text{Co}(\text{NO}_3)_2 \cdot 6\text{H}_2\text{O}]$  and ammonium heptamolybdate  
3  $[(\text{NH}_4)_6\text{Mo}_7\text{O}_{24} \cdot 4\text{H}_2\text{O}]$  with and without the addition of multi-hydroxyl compound. The  
4 loadings of Mo and Co oxides are 18 and 3wt%, respectively. The resultant catalysts  
5 were then dried at 110 °C and calcined at 500 °C for 3 h. The catalysts were then  
6 subjected to sulfidation. Typically, the catalyst was placed in a reactor at 4 MPa of  $\text{H}_2$   
7 and heated to 110 °C. Sulfidizing oil (96% kerosene and 4%  $\text{CS}_2$ ) was then added into  
8 the reactor and maintained for 3 h. Afterwards, the reactor was heated to 360 °C for 8 h.  
9 The resultant catalyst prepared with the addition of multi-hydroxyl compound is named  
10 as Co-Mo-C/mesoporous  $\gamma\text{-Al}_2\text{O}_3$ . For comparison, the catalyst without multi-hydroxyl  
11 compound addition is denoted as Co-Mo/mesoporous  $\gamma\text{-Al}_2\text{O}_3$ .  
12  
13  
14  
15  
16  
17  
18  
19  
20  
21  
22  
23  
24  
25  
26  
27

## 28 2.2 Characterizations

29  $\text{N}_2$  physisorption was performed on a Micromeritics ASAP 2020 instrument at -196  
30 °C. Each sample was heated to 300 °C under vacuum for 3 h prior to testing. The XRD  
31 patterns of the catalysts were determined on a Rigaku Miniflex powder diffractometer  
32 with  $\text{CuK}_\alpha$  radiation ( $\lambda=0.154$  nm). TPR curves were obtained on a Micromeritics  
33 AutoChem 2920 instrument to analyze the reducibility of the catalysts. All samples  
34 were calcined at 450 °C for 1 h and then heated from room temperature to 1000°C in a  
35 10%  $\text{H}_2/\text{Ar}$  mixture. XPS were performed on a Multilab2000X instrument  
36 (ThermoFisher) using  $\text{Mg-K}_\alpha$  radiation. All spectra were corrected using 284.6 eV as the  
37 reference for C1s binding energy. HRTEM measurements were conducted on a JEM-  
38 2100 instrument operating at 200 kV. The sulfur content was obtained by sulfur content  
39 analysis (ANTEK-9000) using Ar and  $\text{O}_2$  as carrier and burning gas, respectively. The  
40 analysis standard was SH/T0689-2000.  $\text{NH}_3$ -TPD was conducted as follows: the  
41 catalysts after calcination were saturated with  $\text{NH}_3$  for 30 min at 100°C. Afterwards, He  
42  
43  
44  
45  
46  
47  
48  
49  
50  
51  
52  
53  
54  
55  
56  
57  
58  
59  
60  
61  
62  
63  
64  
65

1 was flushed to remove the physically adsorbed molecules. The TPD results were  
2 collected in He from 323 to 873 K with a heating rate of 10 K/min. Py-adsorbed IR  
3 spectra were recorded on a PE FTIR Frontier instrument. The system was degassed at  
4 500 °C for 5 h under vacuum and flushed by pure pyridine at room temperature for 20  
5 min. The infrared (IR) spectra were then recorded.  
6  
7  
8  
9  
10

### 11 2.3 Catalytic testing in a 3000 kt/a industrial unit 12 13 14 15

16 The industrial-scale HDS reaction was carried out in a fixed bed reactor, and the  
17 corresponding schematic diagram is illustrated in Fig. 1. Typically, Co-Mo-  
18 C/mesoporous  $\gamma$ -Al<sub>2</sub>O<sub>3</sub> catalyst was shaped into particle with size of 1-3 mm. Both the  
19 top and bottom of the fixed bed reactor were filled with inert particles. The catalysts  
20 were loaded into reactor of  $D/d_p > 18$ ,  $L/d_p > 350$ , where D, L and  $d_p$  are the inner  
21 diameter, height of bed and catalysis particle size, respectively. The feedstock was  
22 pumped into the furnace, and was heated first through heat exchanger. The heated  
23 feedstock was then introduced into the reactor. After reaction, the final products were  
24 separated by high-pressure and low-pressure separators.  
25  
26  
27  
28  
29  
30  
31  
32  
33  
34  
35  
36  
37  
38

39 (Figure 1 should be inserted herein)  
40  
41  
42

## 43 3. Results and discussions 44 45

### 46 3.1 Effect of organic compound on catalyst structure 47 48

49 The mesoporous  $\gamma$ -Al<sub>2</sub>O<sub>3</sub> support in this work was first characterized by N<sub>2</sub>  
50 physisorption, as shown in Fig. 2a. According to the IUPAC classification, it can be  
51 seen that this support has Type IV adsorption-desorption isotherms[1, 21], revealing the  
52 mesoporous characteristic. The hysteresis loop of the isotherm starts at ~0.4, indicating  
53 that the mesopores are intracrystalline rather than intercrystalline. From the inset of Fig.  
54  
55  
56  
57  
58  
59  
60  
61  
62  
63  
64  
65

1  
2  
3  
4  
5  
6  
7  
8  
9  
10  
11  
12  
13  
14  
15  
16  
17  
18  
19  
20  
21  
22  
23  
24  
25  
26  
27  
28  
29  
30  
31  
32  
33  
34  
35  
36  
37  
38  
39  
40  
41  
42  
43  
44  
45  
46  
47  
48  
49  
50  
51  
52  
53  
54  
55  
56  
57  
58  
59  
60  
61  
62  
63  
64  
65

2a, it is observed that the mesoporous  $\gamma$ -Al<sub>2</sub>O<sub>3</sub> support has average pore size (ca. 7.8 nm). The detailed information of pore structure is summarized in Table S1. The pore volume and surface area of mesoporous  $\gamma$ -Al<sub>2</sub>O<sub>3</sub> support are normally larger than those of a typical commercial Al<sub>2</sub>O<sub>3</sub> support. Among the structural and textural properties, pore size is extremely essential because the diffusion of different species inside pores of Al<sub>2</sub>O<sub>3</sub> could affect and limit the HDS overall reaction rate. It is reported that the size of 4,6-DMDBT molecules estimated by molecular orbital calculations is 0.59 × 0.89 nm[22]. This pore size is favorable for the diffusion of the sulfur-containing alkyl derivatives of dibenzothiophene. Based on this mesoporous  $\gamma$ -Al<sub>2</sub>O<sub>3</sub> support, Co-Mo nanoparticles are deposited on support with the addition of the compound. To better show the role of the compound, Co-Mo/mesoporous  $\gamma$ -Al<sub>2</sub>O<sub>3</sub> catalyst without the addition of compound is compared. Fig. 2b shows the XRD patterns of Co-Mo/mesoporous  $\gamma$ -Al<sub>2</sub>O<sub>3</sub> and Co-Mo-C/mesoporous  $\gamma$ -Al<sub>2</sub>O<sub>3</sub> catalyst. Both of the two samples exhibit intense peaks at 46° and 66.8°, which are correlated to the planes (100) and (110) of the  $\gamma$ -Al<sub>2</sub>O<sub>3</sub> phase (JCPDF#29-0063)[23], respectively. There is no low-intensity broad peaks between 16° and 32°, indicating the absence of amorphous Al<sub>2</sub>O<sub>3</sub> phase. For Co-Mo/mesoporous  $\gamma$ -Al<sub>2</sub>O<sub>3</sub> catalyst, there is a peak at 26° which is related to the MoO<sub>3</sub> (021) species. In comparison, no peak shows up at 26° for Co-Mo-C/mesoporous  $\gamma$ -Al<sub>2</sub>O<sub>3</sub> catalyst, indicating that the particles are well-dispersed on support.

(Figure 2 should be inserted herein)

Acidity of a catalyst is a key parameter affecting the HDS performance[24]. For the mesoporous  $\gamma$ -Al<sub>2</sub>O<sub>3</sub> support, there are three kinds of NH<sub>3</sub>-TPD peaks corresponding to different strengths, i.e., weak acidity (150-250°C), medium acidity (250-450°C) and strong acidity (>450°C) [25, 26]. The total acid content includes 36.0% weak acidity,

1 64.0% medium acidity and 0% strong acidity. The total acid content of mesoporous  $\gamma$ -  
2  $\text{Al}_2\text{O}_3$  support is 0.654 mmol/g. After loading CoMo nanoparticles, the Lewis and  
3  
4 Brønsted sites of the two catalysts are determined by Py-IR. The bands at 1445 and  
5  
6 1556  $\text{cm}^{-1}$  are attributed to the pyridine chemisorbed on Lewis sites and the vibration  
7  
8 mode of pyridinium ion adsorbed on Brønsted sites, respectively[27]. In addition, the  
9  
10 pyridine adsorbed on both Lewis and Brønsted sites show up at 1486  $\text{cm}^{-1}$ . The  
11  
12 numbers of sites and B/L ratio of the two catalysts are listed in Table 1. It can be seen  
13  
14 from Table 1 that total acid sites together with B/L ratio are all larger on Co-Mo-  
15  
16 C/mesoporous  $\gamma$ - $\text{Al}_2\text{O}_3$  than those on Co-Mo/mesoporous  $\gamma$ - $\text{Al}_2\text{O}_3$  catalyst, possibly due  
17  
18 to the formation of complex between metal and multi-hydroxyl compound. This could  
19  
20 greatly affect the HDS reaction. It is reported that higher total acidity with larger B/L  
21  
22 ratio could enhance the HDS performance [28]. Therefore, the Co-Mo-C/mesoporous  $\gamma$ -  
23  
24  $\text{Al}_2\text{O}_3$  catalyst is expected to show better HDS activity.  
25  
26  
27  
28  
29  
30

31  
32 (Table 1 should be inserted herein)  
33  
34  
35

36 The interaction between metal and support is then investigated by  $\text{H}_2$ -TPR, which is a  
37  
38 powerful technique to investigate the reduction behavior of supported phases. Fig. 3  
39  
40 shows the  $\text{H}_2$ -TPR spectra of Co-Mo/mesoporous  $\gamma$ - $\text{Al}_2\text{O}_3$  and Co-Mo-C/mesoporous  $\gamma$ -  
41  
42  $\text{Al}_2\text{O}_3$  catalysts. According to Moulijn et al.[29], there is a reduction peak of well-  
43  
44 dispersed molybdenum supported species at low temperature of ca. 450°C. This is  
45  
46 attributed to the partial reduction of Mo(VI) to Mo(IV) of amorphous, highly defective,  
47  
48 multilayered oxides (octahedral Mo species) bounded to  $\text{Al}_2\text{O}_3$  support[30, 31]. It is  
49  
50 clear that the intense peak for Co-Mo-C/mesoporous  $\gamma$ - $\text{Al}_2\text{O}_3$  catalyst is located at  
51  
52 445°C, which is lower than 462.7°C for Co-Mo/mesoporous  $\gamma$ - $\text{Al}_2\text{O}_3$  catalyst,  
53  
54 demonstrating that the interaction between metal and support is weak for Co-Mo-  
55  
56  
57  
58  
59  
60  
61  
62  
63  
64  
65

1 C/mesoporous  $\gamma$ -Al<sub>2</sub>O<sub>3</sub> catalyst. This weak interaction is reported to be beneficial to the  
2 catalytic performance of HDS reaction due to the formation of Co-Mo-S type II sites[2].  
3  
4 Moreover, the absence of additional reduction peaks at 350 °C indicate that Co oxide  
5 supported crystallites is not formed on the supports.  
6  
7

8  
9  
10 (Figure 3 should be inserted herein)  
11  
12

13  
14 To obtain information regarding the morphology and distribution of Co-Mo-S  
15 crystallites, the two catalysts are then analyzed by HRTEM, and the typical HRTEM  
16 images are shown in Fig. 4. Due to the good dispersion of Co, the Co nanoparticles can  
17 not be observed by HRTEM characterization[32]. This is also in accordance with the  
18 XRD results in Fig. 2b. The black thread-like fringes are the Co-Mo-S phase. The  
19 average Co-Mo-S slab length (L) can be calculated from the following equation (3-1):  
20  
21  
22  
23  
24  
25  
26  
27  
28  
29  
30

$$\bar{L} = \frac{\sum_{i=1}^n n_i l_i}{\sum_{i=1}^n n_i} \quad (3-1)$$

31  
32  
33  
34  
35  
36  
37

38 where  $l_i$  is the length of  $i$ th slab,  $n_i$  is the number of particle with a  $l_i$  length. The  
39 statistical results of the length and stacking distributions of Co-Mo-S for the two  
40 catalysts are shown in Table 2. Maximum slab length of Co-Mo-C/mesoporous  $\gamma$ -Al<sub>2</sub>O<sub>3</sub>  
41 catalyst is smaller, and the average length of the slabs on Co-Mo-C/mesoporous  $\gamma$ -  
42 Al<sub>2</sub>O<sub>3</sub> catalyst is 4.8 nm, shorter than the 9.5 nm for Co-Mo/mesoporous  $\gamma$ -Al<sub>2</sub>O<sub>3</sub>  
43 catalyst. In addition, the percentages of Co-Mo-S slabs with 1-2 layers are 75.2 and 47.9%  
44 for Co-Mo/mesoporous  $\gamma$ -Al<sub>2</sub>O<sub>3</sub> and Co-Mo-C/mesoporous  $\gamma$ -Al<sub>2</sub>O<sub>3</sub> catalysts,  
45 respectively. The percentages of 3-5 layers of Co-Mo/mesoporous  $\gamma$ -Al<sub>2</sub>O<sub>3</sub> and Co-Mo-  
46 C/mesoporous  $\gamma$ -Al<sub>2</sub>O<sub>3</sub> catalysts are 20.1 and 49.7%, respectively. The results show that  
47 the addition of compound decrease the interaction between metal and support. Therefore,  
48  
49  
50  
51  
52  
53  
54  
55  
56  
57  
58  
59  
60  
61  
62  
63  
64  
65

1 the average length reduces and the dispersion increases. Moreover, it is reported that the  
2 phase with 3-5 layers is Co-Mo-S type II, which could exhibit superior HDS  
3 performance than Co-Mo-S type I (1-2 layers)[33].  
4  
5

6  
7  
8 (Figure 4 should be inserted herein)  
9

10  
11  
12 (Table 2 should be inserted herein)  
13

14  
15 The surface concentrations of Mo in multiple oxidation states, and the binding  
16 energies of Co and Mo can be determined by XPS, as shown in Table 3. The catalysts  
17 are stored in nitrogen before XPS test to prevent the re-oxidation by air. The typical  
18 curve-fitting of Mo 3d is shown in Fig. S1. The Mo 3d spectra can be divided into three  
19 sets of doublets, which correspond to the Mo<sup>4+</sup>, Mo<sup>5+</sup> and Mo<sup>6+</sup> species[2]. The Mo<sup>4+</sup>  
20 species is usually MoS<sub>2</sub>, which is usually regarded as the active phase[28]. The Mo<sup>5+</sup>  
21 and Mo<sup>6+</sup> species can be attributed to Mo oxy-sulfide and not completely sulfided Mo  
22 species, respectively. From Fig. S1 and Table 3, it is seen that the percentage of Mo<sup>4+</sup> in  
23 the sum of Mo<sup>4+</sup>, Mo<sup>5+</sup> and Mo<sup>6+</sup> species is 75.03% for Co-Mo-C/mesoporous  $\gamma$ -Al<sub>2</sub>O<sub>3</sub>.  
24  
25 In comparison, this value for Co-Mo/mesoporous  $\gamma$ -Al<sub>2</sub>O<sub>3</sub> catalyst is only 65.88%. In  
26 addition, it is also noticed that the Mo binding energy for Co-Mo-C/mesoporous  $\gamma$ -  
27 Al<sub>2</sub>O<sub>3</sub> catalyst is also lower than that for Co-Mo/mesoporous  $\gamma$ -Al<sub>2</sub>O<sub>3</sub> catalyst. The  
28 lower binding energy and higher percentage of Mo<sup>4+</sup> all suggest that the Co-Mo-  
29 C/mesoporous  $\gamma$ -Al<sub>2</sub>O<sub>3</sub> catalyst has weaker interaction between metal and support, and  
30 thus is more easily sulfided, leading to more Co-Mo-S active phases. This finding is  
31 also in accordance with the finding of H<sub>2</sub>-TPR (Fig. 3) and HRTEM (Fig. 4) results.  
32  
33  
34  
35  
36  
37  
38  
39  
40  
41  
42  
43  
44  
45  
46  
47  
48  
49  
50  
51  
52  
53

54  
55  
56 (Table 3 should be inserted herein)  
57

### 58 **3.2 Catalytic performance of Co-Mo-C/mesoporous Al<sub>2</sub>O<sub>3</sub> catalyst**

59  
60  
61  
62  
63  
64  
65

1 The Co-Mo/mesoporous  $\gamma$ -Al<sub>2</sub>O<sub>3</sub> and Co-Mo-C/mesoporous  $\gamma$ -Al<sub>2</sub>O<sub>3</sub> catalysts are  
2 then tested for HDS reaction. The properties of the testing diesel oil are shown in Table  
3  
4 4. The sulfur content for this diesel oil is 9000  $\mu\text{g}\cdot\text{g}^{-1}$ . From table 4, it is seen the diesel  
5 has high sulfur and low nitrogen content, high 95% and FBP, indicating the difficulty of  
6  
7 HDS. The HDS results at different temperature for Co-Mo/mesoporous  $\gamma$ -Al<sub>2</sub>O<sub>3</sub> and Co-  
8  
9 Mo-C/mesoporous  $\gamma$ -Al<sub>2</sub>O<sub>3</sub> catalysts are summarized in Table 5. At 360°C, 6.0 MPa (H<sub>2</sub>  
10  
11 pressure) and 0.77 h<sup>-1</sup>, Co-Mo/mesoporous  $\gamma$ -Al<sub>2</sub>O<sub>3</sub> catalyst shows poor HDS  
12  
13 performance with the product sulfur content of 12  $\mu\text{g}\cdot\text{g}^{-1}$ . In contrast, the Co-Mo-  
14  
15 C/mesoporous  $\gamma$ -Al<sub>2</sub>O<sub>3</sub> catalyst has better performance. The low sulfur content of 7.4  
16  
17  $\mu\text{g}\cdot\text{g}^{-1}$  meets the requirement of Euro V standard. Further increasing the reaction  
18  
19 temperature leads to reduced sulfur contents. The values for Co-Mo/mesoporous  $\gamma$ -  
20  
21 Al<sub>2</sub>O<sub>3</sub> and Co-Mo-C/mesoporous  $\gamma$ -Al<sub>2</sub>O<sub>3</sub> catalysts are 7.0 and 4.0  $\mu\text{g}\cdot\text{g}^{-1}$ , respectively.  
22  
23 Therefore, the temperature for Co-Mo-C/mesoporous  $\gamma$ -Al<sub>2</sub>O<sub>3</sub> catalyst could be 10°C  
24  
25 lower than that for Co-Mo/mesoporous  $\gamma$ -Al<sub>2</sub>O<sub>3</sub> catalyst, which could greatly reduce the  
26  
27 energy consumption.  
28  
29  
30  
31  
32  
33  
34  
35

36 (Table 4 should be inserted herein)

37 (Table 5 should be inserted herein)

38  
39  
40  
41  
42 From the above results, the main reasons for the enhanced performance for Co-Mo-  
43  
44 C/mesoporous  $\gamma$ -Al<sub>2</sub>O<sub>3</sub> support could be the more active Co-Mo-S type II species,  
45  
46 which are originated from weak interaction between metal and support. The higher  
47  
48 activity of Co-Mo-S Type II is generally associated to the high stacking number of slabs  
49  
50 bonding weakly to the support through a small Mo-O-Al linkage[34]. Moreover, it is  
51  
52 also reported that the normal HDS reaction routes[28] include hydrogenation, direct  
53  
54 hydrogenolysis and alkyl transfer desulfurization. Higher B/L ratio and presence of Co-  
55  
56 Mo-S type II species may also lead to better alkyl transfer desulfurization of refractory  
57  
58  
59  
60  
61  
62  
63  
64  
65

1 sulfides such as 4, 6-DMDBT[23, 28]. The ultradeep hydrodesulfurization performance  
2 of Co-Mo-C/mesoporous  $\gamma$ -Al<sub>2</sub>O<sub>3</sub> catalyst is compared with reported catalysts. It can be  
3  
4 seen in Table 6 that the Co-Mo-C/mesoporous  $\gamma$ -Al<sub>2</sub>O<sub>3</sub> catalyst shows a high activity  
5 compared to catalysts reported in the literature[10, 34-38].  
6  
7

8  
9  
10  
11 (Table 6 should be inserted herein)  
12

13  
14 It has been confirmed that Co-Mo-C/mesoporous  $\gamma$ -Al<sub>2</sub>O<sub>3</sub> catalyst has enhanced  
15 performance for HDS reaction. To further verify the stability of this catalyst, the long-  
16 term stability is subsequently evaluated in industrial-scale 3000kt/a plant. The reaction  
17 conditions and results are shown in Table 7 and Fig. 5. The HDS reaction works at low  
18 H<sub>2</sub> pressure P=5.9 MPa, inlet temperature T<sub>i</sub>=350°C, outlet temperature T<sub>o</sub>=362°C,  
19 average temperature T<sub>a</sub>=358°C, hydrogen to oil ratio=308 and space velocity V=0.70h<sup>-1</sup>.  
20  
21 Clearly, the industrial evaluation of Co-Mo-C/mesoporous  $\gamma$ -Al<sub>2</sub>O<sub>3</sub> catalyst also meets  
22 the Euro V requirement of diesel with low sulfur content of 7.8  $\mu\text{g}\cdot\text{g}^{-1}$ . The long-term  
23 evaluation of catalyst at the same reaction condition is shown in Fig. 5. The catalyst  
24 maintains high stability with the low product sulfur content (i.e., smaller than 10  $\mu\text{g}\cdot\text{g}^{-1}$ )  
25 over 5000 h. The reason for the good catalytic stability should be the enhanced mass  
26 transfer ability together with the unique structure of active Co-Mo-S sites.  
27  
28  
29  
30  
31  
32  
33  
34  
35  
36  
37  
38  
39  
40  
41  
42  
43  
44

45 (Table 7 should be inserted herein)  
46

47  
48 (Figure 5 should be inserted herein)  
49

50  
51 It should be noted that the coke formation on Co-Mo-C/mesoporous  $\gamma$ -Al<sub>2</sub>O<sub>3</sub>  
52 catalyst is inevitable due to the contact with carbonaceous feedstock during the long-  
53 term stability test. Therefore, the reaction temperature is normally increased by ca.  
54 0.5°C/month to maintain the quality of products. After long running time, the catalyst  
55  
56  
57  
58  
59  
60  
61  
62  
63  
64  
65



1 should be regenerated. The fresh, used and regenerated catalysts in air at 420°C are then  
2 characterized by N<sub>2</sub> physisorption. Fig. 6 shows that all of the three samples show  
3 similar type IV adsorption-desorption isotherms. The hysteresis loop of the isotherm for  
4 the samples all start at ca. 0.4, indicating that the mesoporous structure is well  
5 maintained. The pore volume of the fresh catalyst is 0.33 cm<sup>3</sup>/g, which decreases to  
6 0.19 cm<sup>3</sup>/g after long-term testing. The regeneration successfully removes the  
7 carbonaceous deposits inside the pores, and increases the pore volume from 0.19 cm<sup>3</sup>/g  
8 to 0.33 cm<sup>3</sup>/g, which is almost the same to fresh catalyst. By using this catalyst, the  
9 3000 kt/a industrial plant in China with the catalyst technique from SINOPEC has been  
10 running smoothly for 3 years. After 3 years, the regenerated catalyst also shows good  
11 HDS performance (Table S2-3). This Co-Mo-C/mesoporous  $\gamma$ -Al<sub>2</sub>O<sub>3</sub> catalyst shows  
12 good performance with the reduced reaction temperature, saving the energy  
13 consumption and greatly increasing the profit. This catalyst is also of referential  
14 importance to the design of industrial catalyst for diesel ultra-deep hydrodesulfurization.  
15  
16  
17  
18  
19  
20  
21  
22  
23  
24  
25  
26  
27  
28  
29  
30  
31  
32

33 (Figure 6 should be inserted herein)  
34  
35  
36  
37

## 38 **4. Conclusion**

39  
40

41 In this work, hydrodesulfurization reaction catalyzed by Co-Mo-C/mesoporous  $\gamma$ -  
42 Al<sub>2</sub>O<sub>3</sub> catalyst at 3000 kt/a industrial-scale is investigated. The sulfur content can be  
43 reduced from 9000 to less than 10  $\mu$ g/g at 5.9MPa (H<sub>2</sub> pressure) and 358°C, meeting the  
44 requirement of Euro V standard. The Co-Mo-C/mesoporous  $\gamma$ -Al<sub>2</sub>O<sub>3</sub> catalyst can even  
45 show 5000 h long-term stability. This performance is much better than Co-  
46 Mo/mesoporous  $\gamma$ -Al<sub>2</sub>O<sub>3</sub> catalyst because the mesoporous  $\gamma$ -Al<sub>2</sub>O<sub>3</sub> support with pore  
47 diameter of 7.8 could facilitates the removal of large sulfide with diffusion limitation  
48 inside the limited pores. In addition, the addition of organic compound leads to  
49  
50  
51  
52  
53  
54  
55  
56  
57  
58  
59  
60  
61  
62  
63  
64  
65

1 increased acidity and weaker metal-support interaction. This enhances the sulfuration  
2 and generates more type II Co-Mo-S active phase. Moreover, the accumulation of coke  
3 during the reaction leads to the reduction of pore volume. Nevertheless, the coke be  
4 effectively removed by regeneration. The results are of essential reference to the design  
5 and development of HDS catalysts.  
6  
7  
8  
9  
10

## 11 **References**

- 12  
13  
14  
15  
16 [1] A. A. Asadi, S. M. Alavi, S. J. Royaei, M. Bazmi, Ultra-deep hydrodesulfurization of feedstock  
17 containing cracked gasoil through NiMo/ $\gamma$ -Al<sub>2</sub>O<sub>3</sub> catalyst pore size optimization, *Energy Fuels* 32  
18 (2018) 2203-2212.  
19  
20  
21  
22 [2] F. Rashidi, T. Sasaki, A. M. Rashidi, A. N. Kharat, K. J. Jozani, Ultradeep hydrodesulfurization  
23 of diesel fuels using highly efficient nanoalumina-supported catalysts: Impact of support,  
24 phosphorus, and/or boron on the structure and catalytic activity, *J. Catal.* 299 (2013) 321-335.  
25  
26  
27 [3] P. A. Nikulshin, A. V. Mozhaev, A. A. Pimerzin, V. V. Kononov, A. A. Pimerzin, CoMo/Al<sub>2</sub>O<sub>3</sub>  
28 catalysts prepared on the basis of Co<sub>2</sub>Mo<sub>10</sub>-heteropolyacid and cobalt citrate: Effect of Co/Mo ratio,  
29 *Fuel* 100 (2012) 24-33.  
30  
31  
32  
33 [4] Y. Chen, H. Song, H. Meng, Y. Lu, C. Li, Z. G. Lei, Polyethylene glycol oligomers as green and  
34 efficient extractant for extractive catalytic oxidative desulfurization of diesel. *Fuel Process. Tech.*,  
35 158 (2017) 20-25.  
36  
37  
38 [5] J. V. Lauritsen, F. Besenbacher, Atom-resolved scanning tunneling microscopy investigations of  
39 molecular adsorption on MoS<sub>2</sub> and CoMoS hydrodesulfurization catalysts, *J. Catal.* 328 (2015) 49-  
40 58.  
41  
42  
43 [6] L. van Haandel, G. Bremmer, E. Hensen, T. Weber, Influence of sulfiding agent and pressure on  
44 structure and performance of CoMo/Al<sub>2</sub>O<sub>3</sub> hydrodesulfurization catalysts, *J. Catal.* 342 (2016) 27-39.  
45  
46  
47 [7] Q. Sheng, G. Wang, Y. J. Liu, M. M. Husein, C.D. Gao, Q. Shi, J. S. Gao. Combined  
48 Hydrotreating and Fluid Catalytic Cracking Processing for the Conversion of Inferior Coker Gas Oil:  
49 Effect on Nitrogen Compounds and Condensed Aromatics. *Energy Fuels* 32(2018) 4979-4987.  
50  
51  
52  
53 [8] T. Fujikawa, H. Kimura, K. Kiriyama, K. Hagiwara, Development of ultra-deep HDS catalyst for  
54  
55  
56  
57  
58  
59  
60  
61  
62  
63  
64  
65

1 production of clean diesel fuels, *Catal. Today* 111 (2006) 188-193.

2 [9] M.H. Zhang, J.Y. Fan, K. Chi, A. J. Duan, Z. Zhao, X.L. Meng, et al., Synthesis, characterization,  
3 and catalytic performance of NiMo catalysts supported on different crystal alumina materials in the  
4 hydrodesulfurization of diesel, *Fuel Process. Tech.* 156 (2017) 446-453.

5 [10] Y. J. Liu, S. Z. Song, X. Deng, W. Huang, Diesel Ultradeep Hydrodesulfurization over  
6 Trimetallic WMoNi Catalysts by a Liquid-Phase Preparation Method in a Slurry Bed Reactor,  
7 *Energy Fuels* 31 (2017) 7372-7381.

8 [11] T. C. Ho, A theory of ultradeep hydrodesulfurization of diesel in stacked-bed reactors, *AIChE J.*  
9 64 (2018) 595-605.

10 [12] W. Chen, X. Long, M. Li, H. Nie, D. Li, Influence of active phase structure of CoMo/Al<sub>2</sub>O<sub>3</sub>  
11 catalyst on the selectivity of hydrodesulfurization and hydrodearomatization, *Catal. Today* 292 (2017)  
12 97-109.

13 [13] S. Boonyasuwat, J. Tscheikuna, Co-processing of palm fatty acid distillate and light gas oil in  
14 pilot-scale hydrodesulfurization unit over commercial CoMo/Al<sub>2</sub>O<sub>3</sub>, *Fuel* 199 (2017) 115-124.

15 [14] O. Klimov, K. Nadeina, Y. V. Vatutina, E. Stolyarova, I. Danilova, E. Y. Gerasimov, et al.,  
16 CoMo/Al<sub>2</sub>O<sub>3</sub> hydrotreating catalysts of diesel fuel with improved hydrodenitrogenation activity,  
17 *Catal. Today* 307(2018)73-83.

18 [15] J. V. Lauritsen, J. Kibsgaard, G. H. Olesen, P. G. Moses, B. Hinnemann, S. Helveg, et al.,  
19 Location and coordination of promoter atoms in Co-and Ni-promoted MoS<sub>2</sub>-based hydrotreating  
20 catalysts, *J. Catal.* 249 (2007) 220-233.

21 [16] J. Chen, J. Mi, K. Li, X. Wang, E. Dominguez Garcia, Y. Cao, et al., Role of Citric Acid in  
22 Preparing Highly Active CoMo/Al<sub>2</sub>O<sub>3</sub> Catalyst: From Aqueous Impregnation Solution to Active Site  
23 Formation, *Ind. Eng. Chem. Res.* 56 (2017) 14172-14181.

24 [17] G. M. Dhar, B. Srinivas, M. Rana, M. Kumar, S. Maity, Mixed oxide supported  
25 hydrodesulfurization catalysts-a review, *Catal. Today* 86 (2003) 45-60.

26 [18] R. Huirache-Acuña, B. Pawelec, E. Rivera-Muñoz, R. Guil-López, J. Fierro, Characterization  
27 and HDS activity of sulfided CoMoW/SBA-16 catalysts: Effects of P addition and Mo/(Mo+ W)  
28 ratio, *Fuel* 198 (2017) 145-158.

29 [19] R. Nava, A. Infantes-Molina, P. Castaño, R. Guil-López, B. Pawelec, Inhibition of CoMo/HMS  
30  
31  
32  
33  
34  
35  
36  
37  
38  
39  
40  
41  
42  
43  
44  
45  
46  
47  
48  
49  
50  
51  
52  
53  
54  
55  
56  
57  
58  
59  
60  
61  
62  
63  
64  
65

1 catalyst deactivation in the HDS of 4, 6-DMDBT by support modification with phosphate, Fuel 90  
2 (2011) 2726-2737.

3  
4 [20] S. A. Ali, S. Ahmed, K. W. Ahmed, M. A. Al-Saleh, Simultaneous hydrodesulfurization of  
5 dibenzothiophene and substituted dibenzothiophenes over phosphorus modified CoMo/Al<sub>2</sub>O<sub>3</sub>  
6 catalysts, Fuel Process. Tech. 98 (2012) 39-44.

7  
8  
9  
10 [21] X. Feng, J. Yang, X.Z. Duan, Y.Q. Cao, B.X. Chen, W.Y. Chen, D. Lin, G. Qian, D. Chen, C.H.  
11 Yang, X.G. Zhou, Enhanced catalytic performance for propene epoxidation with H<sub>2</sub> and O<sub>2</sub> over  
12 bimetallic Au-Ag/Uncalcined TS-1 catalysts, ACS Catal. 8 (2018) 7799–7808.

13  
14 [22] K. S. Triantafyllidis, E. A. Deliyanni, Desulfurization of diesel fuels: Adsorption of 4,6-  
15 DMDBT on different origin and surface chemistry nanoporous activated carbons, Chem. Eng. J. 236  
16 (2014) 406-414.

17  
18 [23] C. Peng, R. Guo, X.C. Fang, Improving ultra-deep desulfurization efficiency by catalyst  
19 stacking technology, Catal. Lett. 146 (2016) 701-709.

20  
21 [24] V. Sundaramurthy, A. Dalai, J. Adjaye, The effect of phosphorus on hydrotreating property of  
22 NiMo/γ-Al<sub>2</sub>O<sub>3</sub> nitride catalyst, Appl. Catal. A: Gen. 335 (2008) 204-210.

23  
24 [25] B. Pawelec, J. Fierro, A. Montesinos, T. Zepeda, Influence of the acidity of nanostructured  
25 CoMo/P/Ti-HMS catalysts on the HDS of 4, 6-DMDBT reaction pathways, Appl. Catal. B: Environ.  
26 80 (2008) 1-14.

27  
28 [26] J. D. de León, T. Zepeda, G. Alonso-Nuñez, D. Galván, B. Pawelec, S. Fuentes, Insight of 1D γ-  
29 Al<sub>2</sub>O<sub>3</sub> nanorods decoration by NiWS nanoslabs in ultra-deep hydrodesulfurization catalyst, J. Catal.  
30 321 (2015) 51-61.

31  
32 [27] C. Kwak, J. J. Lee, J. S. Bae, S. H. Moon, Poisoning effect of nitrogen compounds on the  
33 performance of CoMoS/Al<sub>2</sub>O<sub>3</sub> catalyst in the hydrodesulfurization of dibenzothiophene, 4-  
34 methylthiobenzothiophene, and 4, 6-dimethylthiobenzothiophene, Appl. Catal. B: Environ. 35 (2001)  
35 59-68.

36  
37 [28] X. C. Fang, R. Guo, et al., The development and application of catalysts for ultra-deep  
38 hydrodesulfurization of diesel, Chin. J. Catal. 34 (2013) 130-139.

39  
40 [29] P. Arnoldy, M. Franken, B. Scheffer, J. Moulijn, Temperature-programmed reduction of  
41 CoOMoO<sub>3</sub>Al<sub>2</sub>O<sub>3</sub> catalysts, J. Catal. 96 (1985) 381-395.

42  
43  
44  
45  
46  
47  
48  
49  
50  
51  
52  
53  
54  
55  
56  
57  
58  
59  
60  
61  
62  
63  
64  
65

- 1  
2  
3  
4  
5  
6  
7  
8  
9  
10  
11  
12  
13  
14  
15  
16  
17  
18  
19  
20  
21  
22  
23  
24  
25  
26  
27  
28  
29  
30  
31  
32  
33  
34  
35  
36  
37  
38  
39  
40  
41  
42  
43  
44  
45  
46  
47  
48  
49  
50  
51  
52  
53  
54  
55  
56  
57  
58  
59  
60  
61  
62  
63  
64  
65
- [30] E. Rodríguez-Castellón, A. Jiménez-López, D. Eliche-Quesada, Nickel and cobalt promoted tungsten and molybdenum sulfide mesoporous catalysts for hydrodesulfurization, *Fuel* 87 (2008) 1195-1206.
- [31] L. Pena, D. Valencia, T. Klimova, CoMo/SBA-15 catalysts prepared with EDTA and citric acid and their performance in hydrodesulfurization of dibenzothiophene, *Appl. Catal. B: Environ.* 147 (2014) 879-887.
- [32] S. Eijsbouts, L. Van den Oetelaar, R. Van Puijenbroek, MoS<sub>2</sub> morphology and promoter segregation in commercial Type 2 Ni-Mo/Al<sub>2</sub>O<sub>3</sub> and Co-Mo/Al<sub>2</sub>O<sub>3</sub> hydroprocessing catalysts, *J. Catal.* 229 (2005) 352-364.
- [33] K. Xu, Y. Li, X. Xu, C. Zhou, Z. Liu, F. Yang, et al., Single-walled carbon nanotubes supported Ni-Y as catalyst for ultra-deep hydrodesulfurization of gasoline and diesel, *Fuel* 160 (2015) 291-296.
- [34] F. Rashidi, T. Sasaki, A. M. Rashidi, A. Nemat Kharat, K. J. Jozani, Ultradeep hydrodesulfurization of diesel fuels using highly efficient nanoalumina-supported catalysts: Impact of support, phosphorus, and/or boron on the structure and catalytic activity, *J. Catal.* 299 (2013) 321-335.
- [35] W. Zhou, Q. Zhang, Y. Zhou, Q. Wei, L. Du, S. Ding, et al., Effects of Ga- and P-modified USY-based NiMoS catalysts on ultra-deep hydrodesulfurization for FCC diesels, *Catal. Today* 305 (2018) 171-181.
- [36] S. Shan, H. Liu, Y. Yue, G. Shi, X. Bao, Trimetallic WMoNi diesel ultra-deep hydrodesulfurization catalysts with enhanced synergism prepared from inorganic-organic hybrid nanocrystals, *J. Catal.* 344 (2016) 325-333.
- [37] L. Peña, D. Valencia, T. Klimova, CoMo/SBA-15 catalysts prepared with EDTA and citric acid and their performance in hydrodesulfurization of dibenzothiophene, *Appl. Catal. B: Environ.* 147 (2014) 879-887.
- [38] T. Kabe, W. H. Qian, S. Ogawa, A. Ishihara, Mechanism of Hydrodesulfurization of Dibenzothiophene on Co-Mo/Al<sub>2</sub>O<sub>3</sub> and Co/Al<sub>2</sub>O<sub>3</sub> Catalyst by the Use of Radioisotope <sup>35</sup>S Tracer, *J. Catal.* 143 (1993) 239-248.

**Table Captions:**

**Table 1** Acidity for Co-Mo/mesoporous  $\gamma$ -Al<sub>2</sub>O<sub>3</sub> and Co-Mo-C/mesoporous  $\gamma$ -Al<sub>2</sub>O<sub>3</sub> catalyst.

**Table 2** HRTEM statistic results of Co-Mo/mesoporous  $\gamma$ -Al<sub>2</sub>O<sub>3</sub> and Co-Mo-C/mesoporous  $\gamma$ -Al<sub>2</sub>O<sub>3</sub> catalyst.

**Table 3** XPS results of sulfurized Co-Mo/mesoporous  $\gamma$ -Al<sub>2</sub>O<sub>3</sub> and Co-Mo-C/mesoporous  $\gamma$ -Al<sub>2</sub>O<sub>3</sub> catalysts.

**Table 4** Properties of testing feedstocks for HDS reaction.

**Table 5** Comparison of HDS results for different catalysts.

**Table 6** Comparing the catalytic activity of the Co-Mo-C/mesoporous  $\gamma$ -Al<sub>2</sub>O<sub>3</sub> catalyst and other reported catalysts.

**Table 7** Reaction conditions and results in hydrotreating unit.

1  
2  
3  
4  
5  
6  
7  
8  
9  
10  
11  
12  
13  
14  
15  
16  
17  
18  
19  
20  
21  
22  
23  
24  
25  
26  
27  
28  
29  
30  
31  
32  
33  
34  
35  
36  
37  
38  
39  
40  
41  
42  
43  
44  
45  
46  
47  
48  
49  
50  
51  
52  
53  
54  
55  
56  
57  
58  
59  
60  
61  
62  
63  
64  
65

**Table 1** Acidity for Co-Mo/mesoporous  $\gamma$ -Al<sub>2</sub>O<sub>3</sub> and Co-Mo-C/mesoporous  $\gamma$ -Al<sub>2</sub>O<sub>3</sub> catalyst.

Catalysts	Total acidity ( $\mu\text{mol/g}$ )	Brönsted ( $\mu\text{mol/g}$ )	Lewis ( $\mu\text{mol/g}$ )	B/L ratio
Co-Mo-C/mesoporous $\gamma$ - Al <sub>2</sub> O <sub>3</sub>	544	139	405	0.34
Co-Mo/mesoporous $\gamma$ - Al <sub>2</sub> O <sub>3</sub>	487	44	443	0.10

1  
2  
3  
4  
5  
6  
7  
8  
9  
10  
11  
12  
13  
14  
15  
16  
17  
18  
19  
20  
21  
22  
23  
24  
25  
26  
27  
28  
29  
30  
31  
32  
33  
34  
35  
36  
37  
38  
39  
40  
41  
42  
43  
44  
45  
46  
47  
48  
49  
50  
51  
52  
53  
54  
55  
56  
57  
58  
59  
60  
61  
62  
63  
64  
65

**Table 2** HRTEM statistic results of Co-Mo/mesoporous  $\gamma$ -Al<sub>2</sub>O<sub>3</sub> and Co-Mo-C/mesoporous  $\gamma$ -Al<sub>2</sub>O<sub>3</sub> catalyst.

Properties	Co-Mo/mesoporous	Co-Mo-C/mesoporous
	$\gamma$ -Al <sub>2</sub> O <sub>3</sub>	$\gamma$ -Al <sub>2</sub> O <sub>3</sub>
Maximum slab length (nm)	17.3	11.1
Average slab length (nm)	9.5	4.8
Percentage of 1-2 layers	75.2	47.9
Percentage of 3-5 layers	20.1	49.7
Percentage of >5 layers	4.7	2.4

1  
2  
3  
4  
5  
6  
7  
8  
9  
10  
11  
12  
13  
14  
15  
16  
17  
18  
19  
20  
21  
22  
23  
24  
25  
26  
27  
28  
29  
30  
31  
32  
33  
34  
35  
36  
37  
38  
39  
40  
41  
42  
43  
44  
45  
46  
47  
48  
49  
50  
51  
52  
53  
54  
55  
56  
57  
58  
59  
60  
61  
62  
63  
64  
65



**Table 3** XPS results of sulfurized Co-Mo/mesoporous  $\gamma$ -Al<sub>2</sub>O<sub>3</sub> and Co-Mo-C/mesoporous  $\gamma$ -Al<sub>2</sub>O<sub>3</sub> catalysts.

Catalyst	Co-Mo/mesoporous $\gamma$ -Al <sub>2</sub> O <sub>3</sub>	Co-Mo-C/mesoporous $\gamma$ -Al <sub>2</sub> O <sub>3</sub>
Mo <sup>4+</sup> /(Mo <sup>4+</sup> +Mo <sup>5+</sup> +Mo <sup>6+</sup> ) (%)	65.88	75.03
S/Mo	1.74	1.78
Mo 3d <sub>5/2</sub> BE (eV)	228.8	228.5
Co 2p <sub>3/2</sub> BE (eV)	780.1	778.4

1  
2  
3  
4  
5  
6  
7  
8  
9  
10  
11  
12  
13  
14  
15  
16  
17  
18  
19  
20  
21  
22  
23  
24  
25  
26  
27  
28  
29  
30  
31  
32  
33  
34  
35  
36  
37  
38  
39  
40  
41  
42  
43  
44  
45  
46  
47  
48  
49  
50  
51  
52  
53  
54  
55  
56  
57  
58  
59  
60  
61  
62  
63  
64  
65

**Table 4** Properties of testing feedstocks for HDS reaction.

Feedstock	Diesel oil
Density at 20°C (g/cm <sup>3</sup> )	0.8397
Distillation range (°C)	
IBP (10%)	151/189
30%/50%	242/286
70%/90%	312/352
95%/FBP	366/378
Sulfur content (μg·g <sup>-1</sup> )	9000
Nitrogen content (μg·g <sup>-1</sup> )	150
4,6-DMDBT content (μg·g <sup>-1</sup> )	192

1  
2  
3  
4  
5  
6  
7  
8  
9  
10  
11  
12  
13  
14  
15  
16  
17  
18  
19  
20  
21  
22  
23  
24  
25  
26  
27  
28  
29  
30  
31  
32  
33  
34  
35  
36  
37  
38  
39  
40  
41  
42  
43  
44  
45  
46  
47  
48  
49  
50  
51  
52  
53  
54  
55  
56  
57  
58  
59  
60  
61  
62  
63  
64  
65

**Table 5** Comparison of HDS results for different catalysts.

Feedstock	Diesel oil			
Catalyst	Co-Mo-C/mesoporous $\gamma$ - $\text{Al}_2\text{O}_3$	Co-Mo/mesoporous $\gamma$ - $\text{Al}_2\text{O}_3$		
HDS conditions				
Average reaction temperature ( $^{\circ}\text{C}$ )	360	370	360	370
Hydrogen pressure (MPa)	6.0	6.0	6.0	6.0
Space velocity ( $\text{h}^{-1}$ )	0.77	0.77	0.77	0.77
Hydrogen/oil ratio	400	400	400	400
Sulfur content ( $\mu\text{g}\cdot\text{g}^{-1}$ )	7.4	4.0	12.0	7.0
Nitrogen content ( $\mu\text{g}\cdot\text{g}^{-1}$ )	2.4	2.2	5.0	4.0
4,6-DMDBT content ( $\mu\text{g}\cdot\text{g}^{-1}$ )	4.2	2.5	8.2	4.6

**Table 6** Comparing the catalytic activity of the Co-Mo-C/mesoporous  $\gamma$ -Al<sub>2</sub>O<sub>3</sub> catalyst and other reported catalysts.

Catalysts	Sulfur Concentration (ppm)	Conversion (%)	Temperature(°C)	Stability (h)	Reference
Co-Mo-C/mesoporous $\gamma$ -Al <sub>2</sub> O <sub>3</sub>	9000	99.9	358	5000	This work
CoMoPB/nanoAl <sub>2</sub> O <sub>3</sub>	13500	99.9	350	-	[34]
PGaHUSY	2259	99.7	360	-	[38]
WMoNi-HHD	3904	99.5	360	500	[37]
WMoNi/Al <sub>2</sub> O <sub>3</sub>	-	96.0	360	-	[10]
CoMo/SBA-15	2160	77	3000	-	[36]
Co-Mo/Al <sub>2</sub> O <sub>3</sub>	4000	67	3000	-	[35]

1  
2  
3  
4  
5  
6  
7  
8  
9  
10  
11  
12  
13  
14  
15  
16  
17  
18  
19  
20  
21  
22  
23  
24  
25  
26  
27  
28  
29  
30  
31  
32  
33  
34  
35  
36  
37  
38  
39  
40  
41  
42  
43  
44  
45  
46  
47  
48  
49  
50  
51  
52  
53  
54  
55  
56  
57  
58  
59  
60  
61  
62  
63  
64  
65

**Table 7** Reaction conditions and results in hydrotreating unit.

Catalyst	Co-Mo-C/mesoporous $\gamma$ -Al <sub>2</sub> O <sub>3</sub>	
Diesel	Feedstock	Product
Density at 20°C (g/m <sup>3</sup> )	839.0	831.6
Distillation range (D86, °C)		
IBP/10%	158/191	175/198
30%/50%	233/275	232/274
70%/90	313/349	311/348
95%/FBP	363/367	362/365
Sulfur content ( $\mu\text{g}\cdot\text{g}^{-1}$ )	9000	7.8

**Figure Captions:**

**Fig. 1** Schematic process flow diagram of 3000 kt/a industrial-scale diesel ultra-deep hydrodesulfurization.

**Fig. 2** XRD patterns (a) of mesoporous  $\gamma$ -Al<sub>2</sub>O<sub>3</sub> support and N<sub>2</sub> physisorption (b) of catalysts.

**Fig. 3** H<sub>2</sub>-TPR spectra of Co-Mo/mesoporous  $\gamma$ -Al<sub>2</sub>O<sub>3</sub> and Co-Mo-C/mesoporous  $\gamma$ -Al<sub>2</sub>O<sub>3</sub> catalyst.

**Fig. 4** Typical HRTEM of Co-Mo/mesoporous  $\gamma$ -Al<sub>2</sub>O<sub>3</sub> (a) and Co-Mo-C/mesoporous  $\gamma$ -Al<sub>2</sub>O<sub>3</sub> catalysts (b).

**Fig. 5** Industrial-scale 3000 kt/a stability evaluation (a) in a hydrotreating plant (b).

**Fig. 6** N<sub>2</sub> adsorption-desorption isotherms of fresh, deactivated and regenerated Co-Mo-C/mesoporous  $\gamma$ -Al<sub>2</sub>O<sub>3</sub> catalysts.

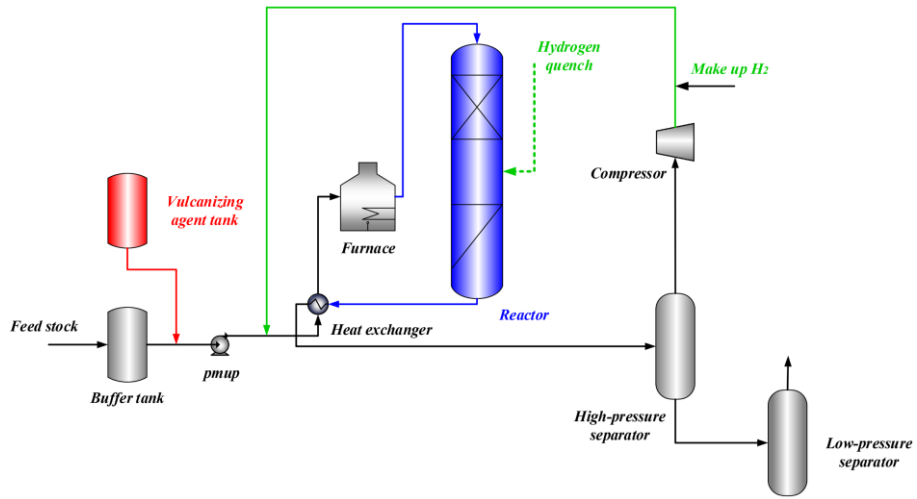


**Fig. 1** Schematic process flow diagram of 3000 kt/a industrial-scale diesel ultra-deep hydrodesulfurization.

1  
2  
3  
4  
5  
6  
7  
8  
9  
10  
11  
12  
13  
14  
15  
16  
17  
18  
19  
20  
21  
22  
23  
24  
25  
26  
27  
28  
29  
30  
31  
32  
33  
34  
35  
36  
37  
38  
39  
40  
41  
42  
43  
44  
45  
46  
47  
48  
49  
50  
51  
52  
53  
54  
55  
56  
57  
58  
59  
60  
61  
62  
63  
64  
65

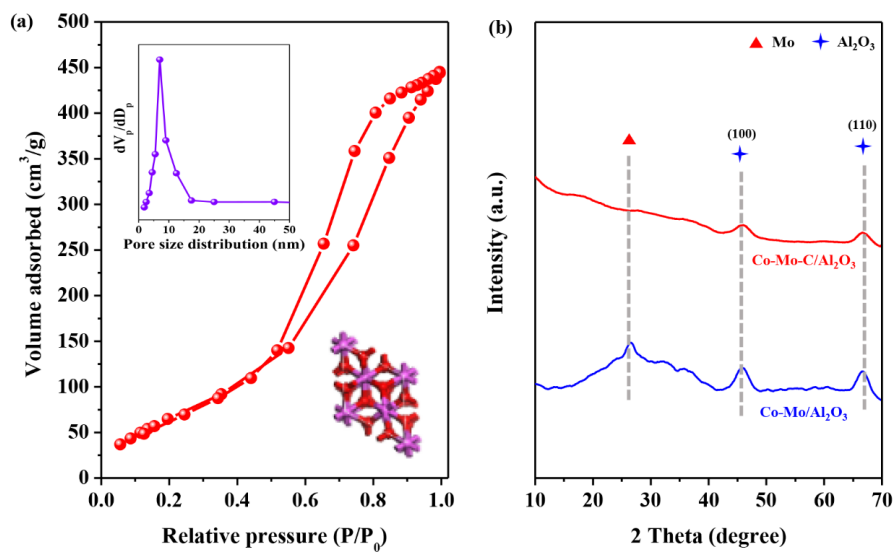


**Fig. 2** XRD patterns (a) of mesoporous  $\gamma$ -Al<sub>2</sub>O<sub>3</sub> support and N<sub>2</sub> physisorption (b) of catalysts.



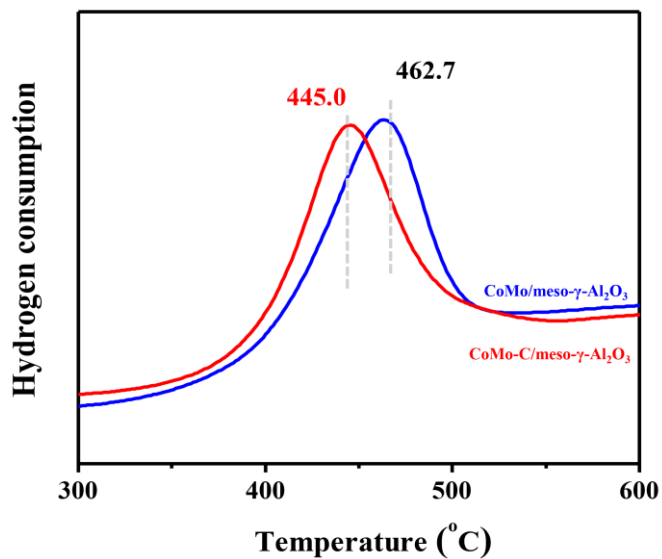


**Fig. 3** H<sub>2</sub>-TPR spectra of Co-Mo/mesoporous  $\gamma$ -Al<sub>2</sub>O<sub>3</sub> and Co-Mo-C/mesoporous  $\gamma$ -Al<sub>2</sub>O<sub>3</sub> catalyst.

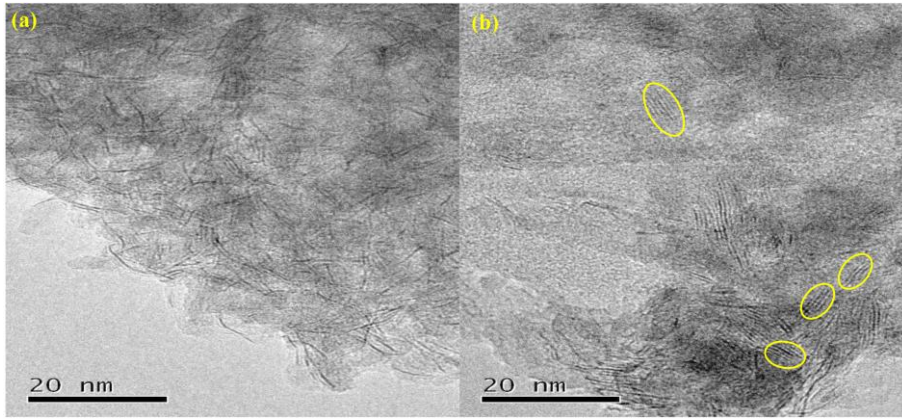


**Fig. 4** Typical HRTEM of Co-Mo/mesoporous  $\gamma$ -Al<sub>2</sub>O<sub>3</sub> (a) and Co-Mo-C/mesoporous  $\gamma$ -Al<sub>2</sub>O<sub>3</sub> catalysts (b).

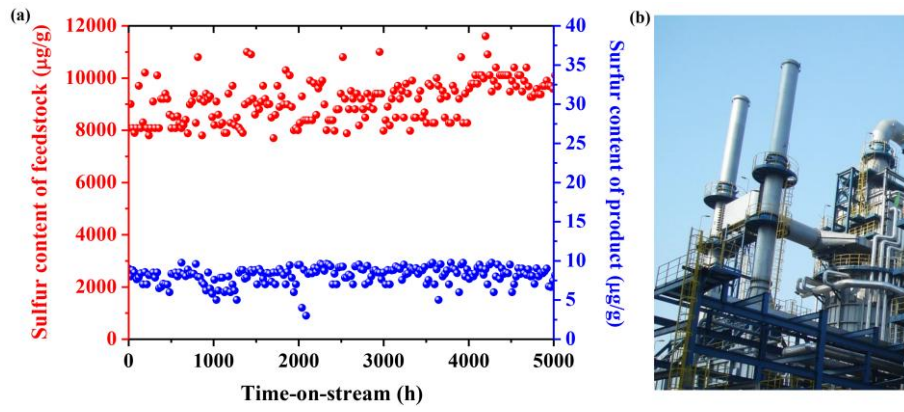


**Fig. 5** Industrial-scale 3000 kt/a stability evaluation (a) in a hydrotreating plant (b).

1  
2  
3  
4  
5  
6  
7  
8  
9  
10  
11  
12  
13  
14  
15  
16  
17  
18  
19  
20  
21  
22  
23  
24  
25  
26  
27  
28  
29  
30  
31  
32  
33  
34  
35  
36  
37  
38  
39  
40  
41  
42  
43  
44  
45  
46  
47  
48  
49  
50  
51  
52  
53  
54  
55  
56  
57  
58  
59  
60  
61  
62  
63  
64  
65

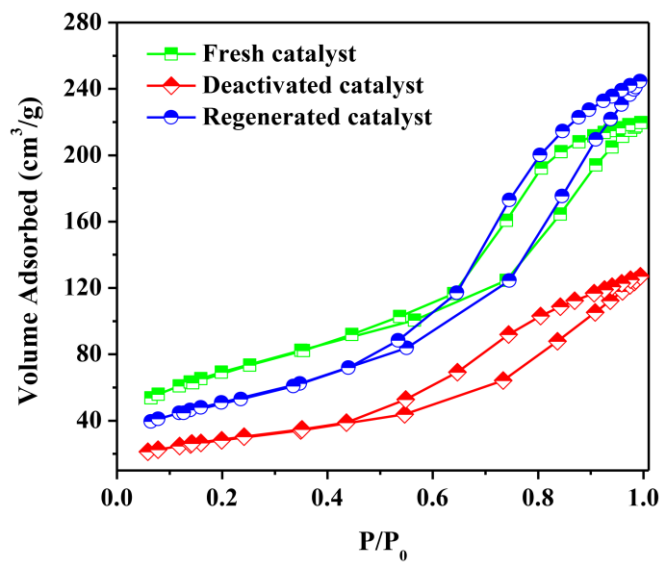


**Fig. 6**  $\text{N}_2$  adsorption-desorption isotherms of fresh, deactivated and regenerated Co-Mo-C/mesoporous  $\gamma\text{-Al}_2\text{O}_3$  catalysts.